Assessment of the Ocean Energy Resources off the South African Coast

April 2013

Ms. I. Meyer

Mr. J. Reinecke

Prof. M. Roberts

Prof. J. L. Van Niekerk

Centre for Renewable and Sustainable Energy Studies

Faculty of Engineering • Fakulteit Ingenieurswese

Private Bag / Privaat Sak X1•Matieland, 7602 • South Africa / Suid-Afrika,

Tel: +27 (0) 21 808 4069•Fax / Faks: +27 (0) 21 808 4277

crses@sun.ac.za

http://www.sun.ac.za/crses

Executive Summary

This report investigates the data available on ocean energy resources and analyses it to determine whether or not the resources available can be utilized to extract energy to generate electricity. There are four distinct sections in this report. The first is an introduction to the subject. The second section discusses what data is currently available, how it was obtained and where it can be found. The third section carries out an analysis of the data from the Agulhas Current to determine the feasibility of harnessing the ocean current energy. Finally, the last section draws conclusions and makes recommendations on further work in this field.

The ocean current and wave data available along the coast of South Africa discussed in section 2 includes the history of these data sets and which commercial entity has the rights to the respective data sets. The instruments used to collect the data and the validity of the data is also presented in this section.

Section 3 of the report focuses on the Agulhas Current, shown to be the only ocean current flanking South Africa that travels swiftly enough to make marine turbine implementation feasible. The Centre for Renewable and Sustainable Energy Studies (CRSES) investigated the statistical properties of the current's measured velocity data, and determined the power that can be generated at three specific locations using a time series analysis. Analysis of the available data highlighted a site just off Cape Morgan (32.507S, 28.831E) as the optimum location for an ocean current turbine plant installation. The site has highest average velocity of 1.5 m/s with reasonable access to the national power grid. In order to determine the resource that can practically be extracted and determine the effects of the variability of the current, a numerical turbine model is used. The collected time series data was run through this model and a capacity factor of 51% was found for the Cape Morgan site.

In the last section the following conclusions are drawn and recommendations made:

- Although there are a number of different data sources and data sets available at this time, there are still many gaps and a lack of coordination between the different stakeholders. It will be very useful if a process can be initiated to bring the different stakeholders together to discuss cooperation and sharing of resources and data. It is recommended that such a process be initiated by one of the interested parties.
- There is clearly a significant amount of energy available in the Agulhas Current but harnessing it remains a technical challenge. The variability of the current, which was greater than what was expected, will also reduce the amount of electricity that can be generated and the attractiveness of the current as a constant (base-load) source of energy. The next step in this investigation will be to consider the available ocean current technology available to generate electricity from this source and to consider how it could be adapted and implemented at one or more of the identified sites. This will need to be done as part of a detailed techno-economic analysis.

Stellenbosch
April 2013

Table of Contents

List of Figures

List of Tables

1. Introduction

The purpose of this report is to investigate the available data on ocean energy resources around South Africa which ultimately can be utilized for the generation of electricity. These resources include both ocean current and ocean wave resources. A range of technologies could be used to harness both current and wave energy. However the focus of this report is not investigating a specific technology, but rather assessing the available resources in order to determine the validity of pursuing ocean power for energy extraction in South Africa.

This report focuses on ocean currents, and a separate report follows detailing a resource assessment on ocean waves. The ocean currents around the world carry great potential for energy extraction and electricity generation. Looking at South Africa (SA) there are two predominant currents which flank the coast line: the one is the Agulhas Current with a Western boundary and the other is the Benguela Current with an Eastern boundary, as shown in Figure 1 below. Figure 1 illustrates the positioning and the flow of these currents and it is seen that the Agulhas Current flows towards the South Pole and the Benguela towards the Equator. It has been proposed that the energy contained in these currents be harnessed to generate electricity. The following report analyses these currents with their available data.

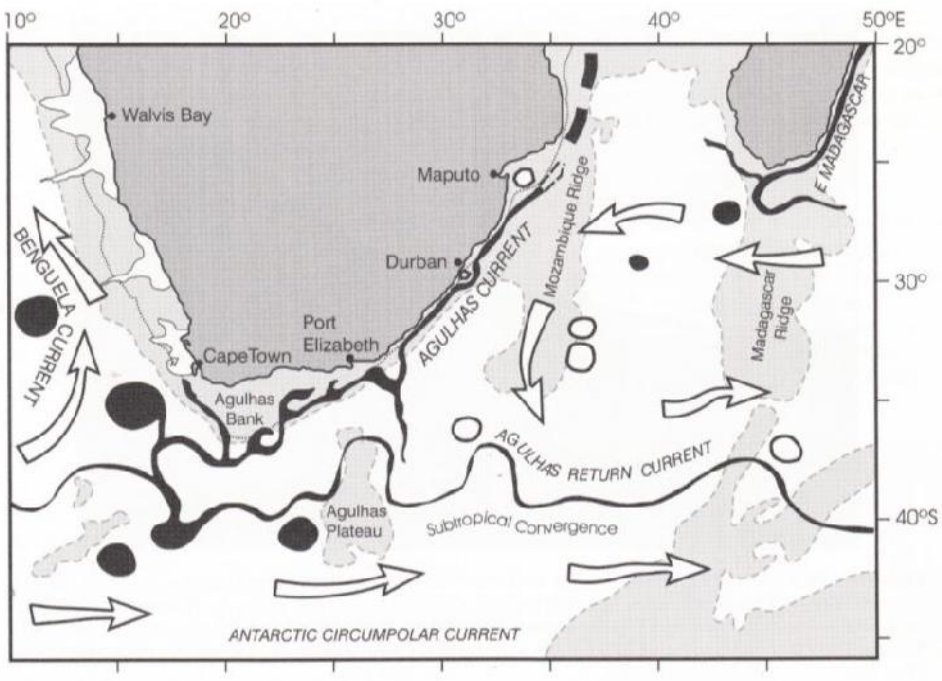

Figure 1: Schematic of ocean currents around South Africa. Areas shallower than 3000 m are shaded; edge of the continental shelf is circumscribed by a 500 m isobaths, indicated by a dotted line. (Lutjeharms, 2006)

2. Overview and assessment of data currently available of ocean current and wave energy

(Section written by Prof. M. J. Roberts)

The objective of this section is to provide an overview and assessment of the currently available data on ocean current and wave energy along the SA coast. The focus of the current assessment will be on the Agulhas Current since it has been found that the Benguela Current has mean flow speeds which

are too low to drive marine turbines. The mean speeds range from 0.11 to 0.23 m/s and transports between 15 and 20 Sv[1] (Gyory, et al., 2012), too low to drive marine turbines and thus the Benguela Current is not be further analysed in this document. The Agulhas Current is stronger than the Benguela Current and it has been found to have approximate transport values of 70 Sv (Bryden, et al., 2005). The report approach is to consolidate all available measured data sets and to determine which are of value to use as input to resource assessments. Data sets and reports comprise of those available in the public domain or released by the owners for the purpose of this project. Other reports and data known to exist by the project team are listed for completeness but the content will not be disclosed without the necessary permissions. Table 1 provides a summary of the data. More detail on each data set is provided later in this section.

Table 1: Overview of available ocean current and wave data in South Africa

	Data set (owned by)	Data set (presented by)	Method	Time period over which data was collected	Range from shoreline	Spatial resolution	Temporal resolution
Ocean current data							
1	CSIR (private)	SADCO	Mainly rotor type	1972 – 2002	1 – 1000 km	208 moorings	
2	Eskom	Eskom	ADCP	2005-10	3 – 30 km	16 moorings	30 min
3	Eskom	Eskom	ADCP	2011–12	5 – 15 km	3 moorings	
Wave data							
4	AVISO	AVISO	Satellite	1991 – present	>60 km	0.5 – 1.0º	
5	NCEP	NOAA	Satellite	1990 - present	>60 km	0.5 – 0.5º	
6	TNPA	CSIR	Wave buoy	1991 – present	~3 km		24 – 0.5 hrs
7	Eskom	Eskom	ADCP	2011–12	1.5 – 80 km		3 hrs

2.1. Ocean currents

2.1.1. Scientific literature

There are a large number of scientific publications on the Agulhas Current. Most of these focus on the trajectory, features and dynamics of this complex current system. These have been summarised in (Lutjeharms, 2006) which a near-complete list of the relevant publications are contained. Since the book's publication, another 52 new studies have been published in leading scientific journals. A first of its kind, the international Chapman Conference was organised in October 2011 at which overviews, new studies and foreseen challenges were presented (De Ruijter et al., 2013). However, in the scientific literature, few publications are concerned with the velocity structures of the Agulhas Current especially on the shelf edge and upper slope, the area most attractive for energy extraction.

2.1.2. Early CSIR studies

Some of the earliest studies on the currents on the east coast of South Africa (i.e. east of Algoa Bay) were undertaken by Whillier (1962) during the expansion of the East London harbour. In these studies, he used surface tracked drogues to investigate the currents within the gentle coastline

[1] A Sv is a Sverdrup, a unit to measure current flow. 1 Sv = 10^6 m^3/s

modulations near East London, and observed small eddies structures with north-eastward coastal currents. This work was followed by two decades of physical oceanography undertaken by the National Research Institute for Oceanology (NRIO) in the 1960s and early 1970s. At first, NRIO concentrated on Natal with recording stations monitored off Durban, Richards Bay and Port Edward using simple techniques, such as ship's drift and ship-derived temperature and salinity profiles. These measurements were complemented by satellite imagery and airborne radiation thermometry (ART) measured from aircraft. Later (between 1976 and 1977), measurements were augmented with rotor-type Aanderaa current meters (model RCM 4) deployed off Richards Bay, Durban, Mzinto and Southbroom (near Port Edward). Schumann (1988) summarized most of this data and noted that currents on the inner regions of the KZN Bight were predominately wind driven and that there were eddy structures smaller than the shelf width on the mid- and outer-shelf. It had also been noted that the Agulhas Current flowed onshore just south of Durban and that a semi-permanent gyre (Schumann 1982) caused a north-eastward current to flow close to the coast off Durban. The Aanderaa current meters deployed off Durban showed that this counter-current flowed for periods of up to seven days, reaching velocities of 100 cm s^{-1}, and extending to the bottom in depths of 230 m. The current meters off Port Edward showed an almost continuous southwestward current close to the coast, with few current reversals.

In 1984, a measurement program was established off East London involving five current meters across the shelf with complementary CTD lines and ART collected at times along the entire East Coast. The current meters deployed just south of the East London Harbour showed that the influence of the Agulhas Current reached the coast on the shelf there. The inshore mooring, deployed 1.3 km from the coast at a depth of 31 m, showed velocity to typically range between 20 cm s^{-1} and 30 cm s^{-1}, reaching up to 60 cm s^{-1}. A mooring farther offshore, 3.5 km from the coast and at a depth of 78 m, showed surface velocities to range up to 95 cm s^{-1}. An onshore current component was noted at both sites, in agreement with the theory of Ekman veering expected in the bottom layer of the Agulhas Current (Schumann 1986), and was thought to be associated with the upwelling found between Port Alfred and East London. Current reversals accounted for some 20% of the data, which appeared to be more common at the inshore site. These currents were barotropic at both sites, i.e. occurring throughout the water column. Only strong southwesterly winds were found to cause current reversals with a one-day time lag, with velocities almost reaching 100 cm s^{-1}. Such events lasted up to four days. However, Schumann (1983) showed earlier that sea level resonates at a similar rate as the weather systems, which could imply that coastal-trapped waves (CTWs) could be responsible for these current reversals as a result of geostrophy. The author also noted that Natal Pulses can lead the Agulhas Current 150 km offshore, and that these may be associated with counter-currents on the shelf.

2.1.3. First Eskom study (2003)

With the growing interest worldwide in the exploitation of marine renewable energy resources, Eskom became interested in generating electricity from the Agulhas Current. It commissioned a preliminary study (CSIR, 2003) to inform subsequent pre-feasibility and feasibility studies, and its consultants to assess the potential for power generation from ocean currents offshore of South Africa. The approach was broad, entailing searches and summaries of data and literature at the time on the bathymetry, bedforms, sediment transportation and ocean currents along the east coast. In addition to these, the potential economic and engineering design constraints and potential environmental impacts constraints were also summarised.

With respect to the objectives of this report, the most important part of that feasibility study was the provision of an overview of ocean currents around the South African coast with a special focus on the Agulhas Current. For completeness, the Eskom study included mention of ship-borne and mooring measurements, satellite-tracked buoys, remote sensing (infrared and altimetry) and hydrodynamic models. However, it was quickly acknowledged that the latter three methods (at the time of this feasibility study) had little to contribute to providing actual data on the velocity of the Agulhas Current. This is currently and continually changing, as advances in satellite sensors and signal analyses progress.

Regarding ship-borne measurements, the report recommended only those taken by research vessels, those collected by the CSIR, Marine and Coastal Management (MCM), and international vessels. In the latter case, 5 cruises of relevance in the area have been conducted by Toole and Warren, 1993; Beal and Bryden, 1997, 1999; and Donohue et al., 2000. In all cases, a lowered-ADCP was used to reveal the vertical and horizontal velocity structure of the Agulhas Current. These results have been published but the data is not available in South Africa. Roberts et al. (2010) published S-ADCP data between Port Edward and East London. This data only goes to a depth of 600 m and is available on request.

An overview of current meter records (totaling 208 up until 2002) on the east coast had been provided by Eskom. All of these were available in the SADCO database but many required permission for use as they were collected for CSIR contracts. It is also important to note that data had only been collected at shallow levels (i.e. < 50 m). Owing to the rotor-type technology used, most deployments were of short duration (a few months) mainly as a result of the rotor-type current meter subject to bio fouling. Mainly due to the readings being too shallow(the meter placement was incorrect) thus none were actually analysed. Instead, data was taken from the literature – in particular from Duncan (1976) (see Figure 2) where it is shown that the core of the Agulhas Current is closest to the coast off Cape St Lucia and Port Edward, and remains close inshore until East London. According to these early studies, the mean velocities increase from Port Edward, southwards, to a maximum velocity off East London.

The study concluded the most viable locations for power generation from ocean currents are along the east coast of South Africa, off Port Edward, and in an offshore region stretching from the Mbashe River southwards to East London. Available data indicate that mean near-surface speeds of up to 1.5 m s^{-1} or more occur at these preferred locations in water depths of between 200 m and 500 m approximately 12-30 km offshore. Maximum speeds at these locations are known to exceed 2.5 m s^{-1}. It further recommended that Eskom commission a current measurement program at the preferred locations with the deployment of current meters between 500 and 1 000 m, along with shore-normal ship based transects through the currents.

a)

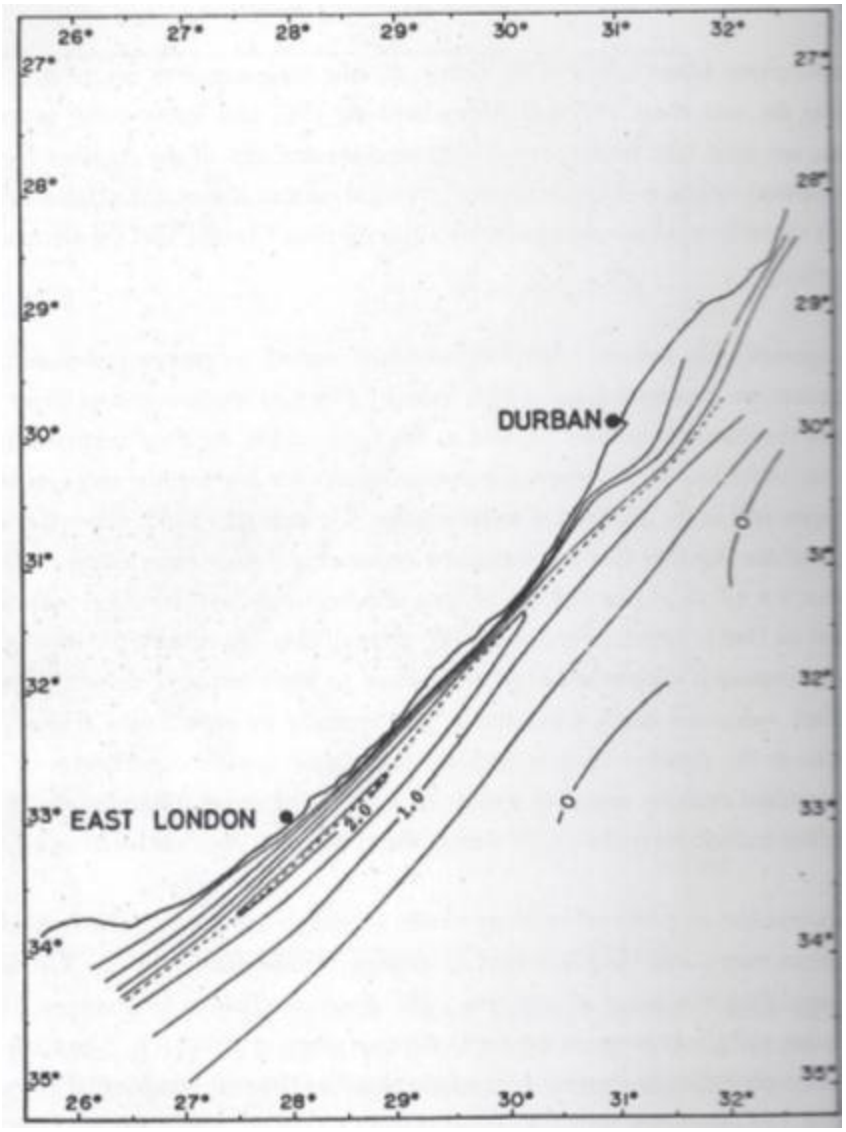

b)

Location		Water depth				
		100 m	200 m	300 m	500 m	1000m
Richards Bay	Current speed (m/s)	0.7	0.8	0.9	1.0	1.1*1
	Distance offshore (km)	20	23	25	26	38
Durban	Current speed (m/s)	-0.1	-0.1	-0.1	0.6	1.0*2
	Distance offshore (km)	9	12	14	35	60
Port Edward	Current speed (m/s)	1.3	1.5	1.5*3	1.5*3	1.4
	Distance offshore (km)	11	12	14	17	20
East London	Current speed (m/s)	1.2	1.4	1.4	1.3	1.2*4
	Distance offshore (km)	21	24	26	30	34
Port Elizabeth	Current speed (m/s)	0.8	1.2	1.2	1.1	1.2
	Distance offshore (km)	9	44	46	55	58

*1 The surface current core (> 1.2 m/s) off Richards Bay lies inshore of the 1000 m isobath.

*2 The surface current core (> 1.1 m/s) off Durban lies inshore of the 1000 m isobath.

*3 The surface current core (> 1.5 m/s) off Port Edward is located at water depths of between 300 m and 1000 m

*4 The surface current core (> 1.3 m/s) off East London lies inshore of the 1000 m isobath.

Figure 2: (a) Lines of constant speed in m s-1 within the Agulhas Current off the southeast coast (from Duncan, 1976). The dashed line indicates the axis of maximum speed. (b) Summary table of mean velocities calculated from available current meter deployments as a function of depth and location. Distance offshore is also given. Data sourced from the SADCO between 1972 and 2002.

2.1.4. Second Eskom *in situ* east coast study (2005-2010)

Deployments and available data

The CSIR preliminary study was followed by an *in situ* validation study. Under the supervision of Eskom, a series of 16 ADCP deployments (referred to as experiments) were deployed along the east coasts between Port Edward and Port Alfred between September 2005 and September 2010 (Figure 3). Details of these deployments are given in Table 2. Full metadata for this study can be found in Appendix A. At two sites, moorings were placed in shallower water on the shelf to investigate shoreward velocities. The first deployment (E1, E2, and E3) comprised a trans-shelf line of 3 moorings. The remainder of the deployments were mostly singular along the shelf edge (~100 m).

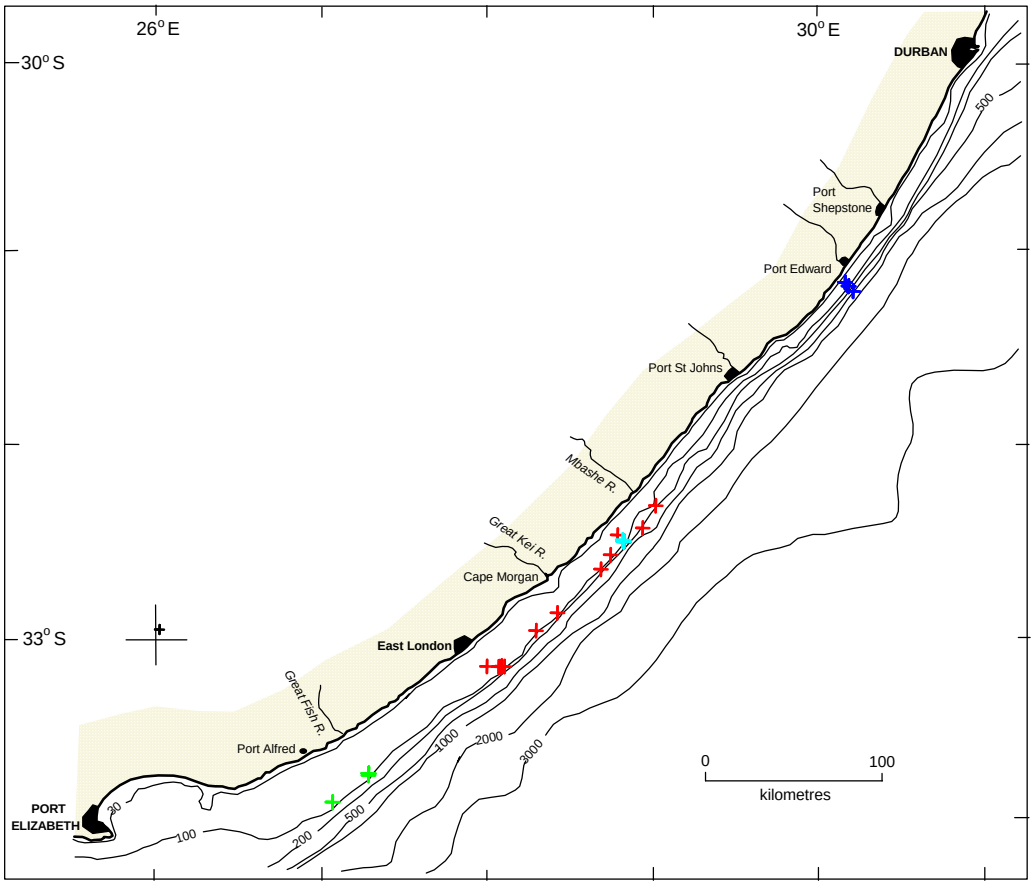

Figure 3: Positions of the deployments considered in this report. The dark blue crosses in the north refer to the deployments off Port Edward (PE in Table 2), the red crosses are those deployments labelled EL in Table 2, the light blue crosses are labelled CM and the green are labelled FR.

Table 2: Details of the ADCP deployments for the 16 experiments: the number in the "ADCP type" refers to the frequency of the instrument, while those instruments with no pressure sensor are indicated with a (~~P~~)

Experiment & Filename		ADCP type	Deployment date	Recovery date	Water depth (m)	Latitude °S	Longitude °E
	PE601	RDI 600	2005/09/08	2005/12/11	36.8	31.17855	30.15253
E1	PE301	RDI 300	2005/09/08	2005/12/11	65.0	31.19722	30.17517
	PE751	RDI 75	2005/09/08	2005/12/11	161.0	31.22263	30.20273
	PE602	RDI 600 (~~P~~)	2005/12/11	2006/04/10	38.0	31.17860	30.15263
E2	PE302	RDI 300	2005/12/11	2006/04/10	66.7	31.19732	30.17480
	PE752	RDI 75	2005/12/13	2006/04/06	178.4	31.22303	30.20270
	EL901	Nortek	2005/12/14	2006/04/07	88.3	32.50997	28.83000
	PE603	RDI 600	2006/04/10	2006/09/09	37.1	31.17865	30.15245
E3	PEM03	RDI 600 (~~P~~)	2006/04/10	2006/09/09	67.1	31.19753	30.17460
	EL303	RDI 300	2006/04/11	2006/09/02	101.0	32.32363	29.02225
	EL902	Nortek	2006/04/11	2006/09/02	88.0	32.50717	28.83242
E4	EL403	RDI 75	2006/05/01	2006/09/08	101.0	32.96595	28.30622
	EL903	Nortek	2006/09/08	2006/12/12	89.8	32.50763	28.83210
E5	EL304	RDI 300	2006/09/08	2006/12/12	95.0	32.47545	28.79237
	EL754	RDI 75	2006/09/08	2006/12/12	97.0	32.57633	28.75208
	EL904	Nortek	2006/12/13	2007/03/07	86.3	32.50753	28.83292
E6	EL755	RDI 75	2006/12/13	2007/03/07	107.0	32.64985	28.69545
	EL305	RDI 300	2006/12/13	2007/03/07	93.8	32.87433	28.43367
	EL756	RDI 75	2007/03/08	2007/08/17	201.0	32.43732	28.94465
E7	EL905	Nortek	2007/03/08	2007/08/17	90.5	32.50743	28.83293
	EL306	RDI 300	2007/03/08	2007/08/14	103.7	33.15012	28.11602
	EL906	Nortek	2007/08/18	2007/12/06	89.8	32.50735	28.83287
E8	EL757	RDI 75	2007/08/18	2007/12/06	88.9	32.51000	28.83287
	EL307	RDI 300	2007/08/18	2007/12/06	88.5	33.15005	28.09953
	FR301	RDI 300	2007/08/18	2007/12/05	94.6	33.85170	27.08120
	EL907	Nortek	2007/12/07	2008/03/30	90.0	32.50802	28.83293
E9	EL308	RDI 300	2007/12/07	2008/03/30	90.0	33.14983	28.09905
	FR752	RDI 75	2007/12/08	2008/03/29	93.0	33.85070	27.08023
	EL908	Nortek	2008/04/01	2008/05/04	92.0	32.50754	28.83314
E10	EL309	RDI 300 (~~P~~)	2008/04/01	2008/07/11	93.7	33.14990	28.09933
	FR303	RDI 300	2008/04/01	2008/06/27	102.0	33.70283	27.29817
	EL909	Nortek	2008/07/12	2008/08/14	89.5	32.50495	28.83143
E11	CM301	RDI 300	2008/07/11	2008/12/10	87.7	32.50737	28.83185
	EL310	RDI 300	2008/07/12	2008/12/13	87.0	33.14970	28.09903
	FR304	RDI 300 (~~P~~)	2008/07/13	2008/12/09	101.0	33.70290	27.29782
	CM302	RDI 300	2008/12/13	2009/03/23	91.0	32.49923	28.82348
E12	EL910	Nortek	2008/12/13	2009/01/13	91.0	32.50560	28.83183
	EL311	RDI 300	2008/12/12	2009/03/23	88.1	33.15115	28.09700
	FR305	RDI 300 (~~P~~)	2008/12/12	2009/02/04	96.7	33.70310	27.29803
	CM303	RDI 300	2009/03/23	2009/08/25	88.7	32.50638	28.83150
E13	EL312	RDI 300	2009/03/23	2009/08/26	91.6	33.15160	28.08072
	FR306	RDI 300 (~~P~~)	2009/03/21	2009/08/24	96.5	33.70322	27.29727
	CM304	RDI 300 (~~P~~)	2009/08/25	2009/12/05	88.0	32.50790	28.83100
E14	EL313	RDI 300	2009/08/26	2009/12/04	87.7	33.15203	28.08727
	FR307	RDI 300	2009/08/26	2009/12/04	96.3	33.70333	27.29677
	CM305	RDI 300 (~~P~~)	2009/12/05	2010/03/03	90.9	32.50733	28.83183
E15	EL314	RDI 300	2009/12/04	2010/03/03	94.0	33.15145	28.00866
	FR308	RDI 300	2009/12/04	2010/03/04	98.3	33.70335	27.29750
	CM306	RDI 300 (~~P~~)	2010/03/03	2010/09/13	89.0	32.50725	28.83179
E16	EL315	RDI 300	2010/03/03	2010/09/13	93.0	33.15140	28.08651
	FR309	RDI 300	2010/03/04	2010/09/03	93.7	33.71332	27.29745

ADCP measurement technology and collected data

The current measurements all employed the acoustic Doppler principle: transducer transmits an acoustic signal into the water column, and current velocity is then calculated from measured frequency changes in the return pulse. Reflected pulses from pre-determined layers (called bins) throughout the water column can be recorded and processed, resulting in the acquisition of the vertical velocity structure. A limitation of ADCP technology is that they cannot measure close to the sea surface due to inference caused by air bubbles. Equipment from two different manufacturers were used, namely *Teledyne RDI* and *Nortek* with frequencies ranging from 75 to 600 kHz depending on the depth of the site. Details of the instruments themselves and the operational depth range can be obtained from the manufacturers' websites http://www.rdinstruments.com/ and http://www.nortek-as.com/en).

The water depth in most of the deployments in Table 2 is taken to be the sounding made by the ship at the time of deployment with the addition of 5m to account for the draft of the ship. This is the value given in the reports. The mooring configuration is shown in Figure 4.

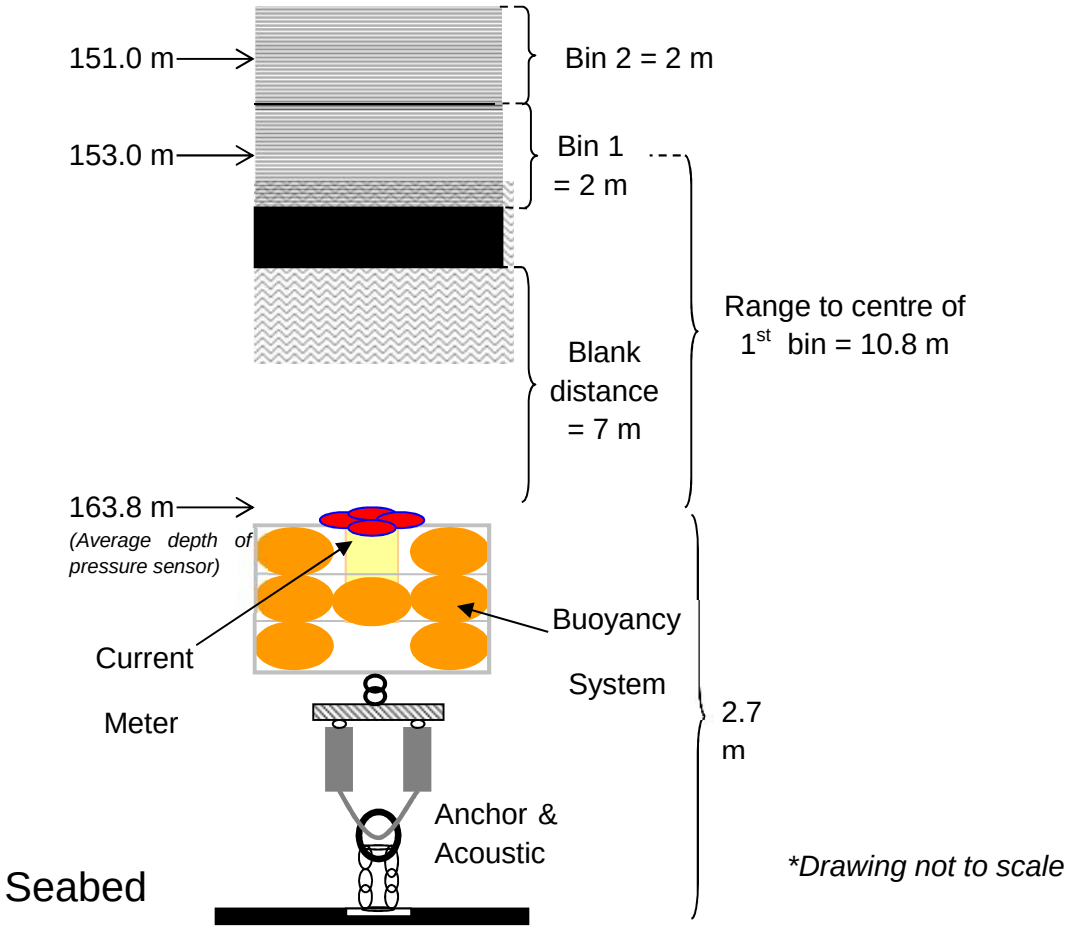

Figure 4: Mooring configuration showing the anchoring structure on the seabed, the buoyancy system (orange ellipses) and the position of the ADCP current meter and the transducer heads and pressure sensor. The distances shown apply to mooring PE751, and are given as an example.

The distances in Figure 4 are given for the mooring PE751 in a water depth of 167 m. For the shallower instruments, the height of the pressure sensor above the seabed is reduced to 2.3 m. Owing to technical constraints (i.e. the blanking distance), current measurements only start at a given distance above the transducers (and pressure sensor), and vary from 10.8 m for the deeper,

lower frequency meters to 3.1 m for the higher frequency, shallower meters. For the majority of moorings the distance from the transducers to the centre of the first bin is about 4.5 m with a chosen bin size of 2 m. The number of bins (resolution of measurement in the water column) varied from 20 to 90. The data interval was set at either 30 minutes or 60 minutes, and the recorded value was then the mean current velocity measured in each bin over this period.

There is a remarkable amount of data available from all the current meter deployments. The analyses, which included a large number of statistics, enabled several conclusions to be reached — namely:

1. As expected, the dominant currents measured throughout the whole programme were those associated with the Agulhas Current flowing essentially parallel to the coastline and isobaths in a southwestward direction. There is a corresponding increase in current speed throughout the water column with distance offshore, and consequently there is a need to assess the optimal distance from the coast for a turbine. There are increases in cost with distance and with depth, but these results indicate that a position near the shelf break (about 90 to 100 m depth) may present the best option.
2. There is significant vertical structure in the currents with the bottom boundary layer extending through much of the water column on the shallower shelf. There is a corresponding marked decrease in current speed with depth, and also Ekman veering is prominent near the seabed. It was therefore assumed that the optimum position for a turbine would be as close as possible to the surface. However, the drafts of the big ships can be as much as 20 m, while shallower than this also brings with it greater impact of surface waves and the effect of wind. Assuming a turbine diameter of around 30 m, means that much of the analyses was based on the 20 to 50 m depth range.
3. The ADCP deployments were made on the coastal area stretching from Port Edward to the Fish River with a greater concentration on the southern section once it became apparent that currents off Port Edward were not as favourable as farther south. With the establishment of the Agulhas Current south of Durban and the propagation southward of Natal Pulses and smaller-scale meanders, the widening shelf southwards and the propagation of continental shelf waves from the south, there is considerable variability along the coast.
4. For the analysis, four regions were identified and grouped, namely Port Edward, immediately south of the Mbashe River, north and off East London, and off the Fish River. The results indicate that current speeds increase southward from Port Edward, while south of East London the widening shelf means that suitable currents are farther offshore. Nonetheless, off the Fish River the current structures were also not as suitable as farther north. Consequently the area between the Mbashe River mouth and East London appears to have the most suitable currents, with the grouping south of Mbashe being preferable.
5. However, it is important to realise that current reversals do occur on a regular basis, probably as a result of meanders in the Agulhas Current, or a large *Natal Pulse* moving south from the northeast. In the south, current reversals also occur as a result of coastal trapped waves moving north past Port Elizabeth, although these are attenuated by the Agulhas Current. A duration curve for Mbashe shows that over the 57-month record, currents less than 0.5 $m.s^{-1}$ (including reversals) and lasting for at least 5 days, occurred about once every two months. In total, current speeds less than 0.5 ms^{-1} (or reversals) occurred 15.5% of the time. On the other hand, current speeds greater than 1.5 m s^{-1} occurred for 35.5% of the record with approximately one event every two

months lasting longer than 5 days. Current speeds between 1.2 and 1.5 m s^{-1} were measured for 27.2% of the time.

6. It is important to realise that a more detailed analysis is required to clarify the impact of meanders, *Natal Pulses* and coastal-trapped waves. In particular, it is probable that not every meander or *Natal Pulse* will cause current reversals – since the definition of such pulses is subjective in any case - and certainly many coastal trapped waves will be too small to have a large enough impact to cause a current reversal. There will also be differences in the extent of the slow-down of current speeds, or of complete reversals, across the shelf. Particular events can be analysed in more detail using satellite imagery, while coastal-trapped waves, are correlated with winds and variations in sea level at the coast.
7. Nonetheless, because of the large-scale nature of the Agulhas Current, a predictive capability for current reversals, or even current speed decreases, associated with meanders and *Natal Pulses* should be possible using satellite imagery. Thus these features progress slowly southwestwards along the coast at speeds around 20 cm s^{-1} – or just less than 20 km day^{-1} - and are easily identified in the imagery. While details of the effects of the meanders and pulses still need further investigation, lead times of days or even a week should be possible. Predicting the effects of coastal-trapped waves will be more difficult, since it will involve the real-time acquisition and analysis of wind and sea level data.

2.1.5. Third (Cape Morgan) Eskom study (2012)

The second exploratory Eskom study concluded that the highest velocities relative to the shelf break (100 m) occur between the Mbashe River and East London. Eskom initiated a study in 2012 to collect 12 months of velocity and direction data across the shelf near Cape Morgan spanning the depths 60 – 250 m using three ADCP moorings. These data are collected half hourly and at the time of the report had not been processed.

2.1.6. ASAR current measurements

The majority of this subsection has been based on the publication *Mapping the Agulhas Current from Space: An assessment of ASAR surface current velocities* authored by M. J. Rouault, A. Mouche, F. Collard, J.A. Johannessen and B. Chapron.

Background

A major problem with moored current meters in the form of rotor-types and ADCPs is that they measure the velocity and direction of flow at a specific site, albeit the latter does provide water column profiles. Ship-borne ADCPs provide horizontal and vertical measurements along tracks but the technique suffers from the slowness of the collection method and that the data may not necessarily truly reflect a synoptic view of the current field. Satellites on the other hand do provide synoptic views of the ocean. In particular, altimetry through the use of the geostrophic approximation has enabled scientists to estimate the upper transport and magnitude of the major ocean currents, track eddies or even discover new currents. Closer to the shore however, altimetry suffers from serious limitations due to factors such as land contamination, atmospheric errors or inaccuracies in the estimation of the mean dynamic topography (MDT) — all of which result in t loss of data typically 50 km from the coast (Vignudelli et al., 2008; Madsen et al., 2007). Space-borne radar, however, can directly measure surface ocean currents but it is a new and developing technology. The Real Aperture Radars (RAR) and Synthetic Aperture Radars (SAR) used are side-looking radars which illuminate the ocean surface in a direction perpendicular to the flight line but within an area defined by the radar footprint. (Note: SARs were designed to improve on the resolution of RARs). Along the satellite path (in the azimuth direction), echoes returned from the

radar pulses are recorded, processed and converted to digital data to produce a two dimensional image of the ocean surface. SARs are the only instruments in space that can simultaneously provide direct measurements of surface current, wave and wind fields. The main challenge with the analysis of SAR data for oceanography lies in adequately separating the different oceanographic signatures observed in the images of the sea surface roughness.

Methodology and data

Chapron et al. (2004) proposed the first technique to extract surface current information from SAR data so as to synoptically map ocean currents from the open ocean to the coast at a high resolution. His method, commonly referred as the *Doppler shift method*, relies on the careful analysis of the Doppler centroid anomaly. The anomaly accounting for the motion of surface roughness elements on the ocean surface corrected for the rotation of the earth. The principle of surface current measurements from the (Advanced) Synthetic Aperture Radar (ASAR) is similar to that of land-based radar measurement systems and involves the extraction of a line of sight velocity from information contained in the frequency spectrum of the returned radar echoes. This can then be projected onto a horizontal plane to provide a range-directed surface current velocity. With precise information on the satellite's orbit and the antennae's attitude, it is possible to very accurately remove the effect of the motion of the satellite relative to the Earth from the Doppler spectrum. Over the ocean, the resulting Doppler anomaly thus contains information solely related to the motion of the sea surface roughness elements which reflects the combined action of the wind, waves and current motions. Previous studies using interferometry have demonstrated the ability of SARs to measure surface currents from airborne platforms (Goldstein and Zebker, 1987; Shemer et al., 1993; Romeiser et al., 2005).

The technique of Chapron et al. (2004) is based on using a single SAR antenna. Using this method and the Doppler centroid, estimates provided by the European Space Agency (ESA) in the metadata set of ASAR Wide Swath Medium (WSM) resolution images (Madsen, 1989; Chang and Curlander, 1992) (http://envisat.esa.int/handbooks/asar/CNTR2-6.htm#eph.asar.prodalg.levb.alg.descr.dopfreq), the radar division of Collecte Localisation Satellites (CLS) now processes all ASARWSM images acquired over the Agulhas Current region on a systematic basis (Collard et al., 2008; Johannessen et al., 2008). For each ASARWSM acquisition, the Doppler centroid anomaly is extracted from the total Doppler centroid using a geometrical model. The Doppler centroid anomaly is then further processed to compensate along-track large cross section variations (induced by instrumental or signal processing errors) using land surface references. State of the art radar imaging models are required to precisely account for the relative influence of the wind, waves and currents on the mean motion of the sea surface roughness elements and its associated Doppler anomaly. The derivation of surface current velocities from the Doppler centroid anomaly can therefore be summarised as a 3-step process: 1) Calculate the Doppler centroid anomaly by removing the relative motion of the satellite to the Earth, 2) Remove the wind-induced contributions from the total Doppler centroid anomaly and, 3) Convert the Doppler centroid anomalies to range-directed surface velocities. The ASAR derived velocity is the absolute surface current velocity across the track of the satellite, with positive values indicating a flow moving away from the radar. Velocities derived from the ASAR dataset are referred to as the ASAR range velocities.

The Agulhas Current — the world's strongest western boundary current — has provided an ideal natural laboratory to test new remote sensing products such as the ASAR range-directed surface current velocities (referred to as a supersite by ESA). Since July 2007, maps of surface current velocities in the Agulhas Current region have been systematically recovered from the Doppler shift

measurements of the Envisat ASAR under the ESA funded SAR ocean wind-wave-current project (Collard et al., 2008; Johannessen et al., 2008). The ASAR range velocity product has a resolution of about 4 km in range and 8 km in azimuth (Collard et al., 2008). Over the Agulhas Current region, one descending (morning) and one ascending (evening) ASAR WSM image has been obtained every 3.5 days since July 2007. Near real time range-directed surface current velocities derived from ASAR are freely available for download on the soprano website (http://soprano.cls.fr). The sampling of ASAR range velocities over the Agulhas Current region is not homogeneous, with most of the satellite's image acquisitions occurring between East London and Cape Agulhas (20°E to 28°E).

Accuracy of ASAR

Previously Collard et al. (2008) have shown promising results with range-directed surface current velocities with an RMS error equivalent to about 0.2 m s^{-1}. However, comparisons between ASAR- and drifter-derived range velocities by Rouault et al (2010) showed that inaccuracies in the magnitude of ASAR surface current velocities occur when erroneous wind fields are used for the removal of the wind induced drift on the overall surface motion. The impact of inaccurate wind fields is particularly pronounced at low radar incidence angles i.e. <30°. From 4215 co-locations obtained mainly in the Agulhas Return Current region, the mean bias and RMS error between the ASAR and drifters range velocities were equal to 0.13 m s^{-1} and 0.56 m s^{-1}, respectively. Rain was also found to negatively impact the ASAR measurements causing outlier data with deviations from the mean sometimes in excess of 4 m s^{-1}.

The uncertainty in ASAR measured velocities presently is perhaps best illustrated in Figure 5 from Rouault et al. (2010) which depicts a time series of ASAR and altimetry (AVISO) range-directed surface current velocities extracted at a location in the mean position of the Agulhas Current core offshore Port Elizabeth (25.8°E; 34.7°S). This time series was derived using all ASAR ascending path observations when the surface velocity measured by the ASAR is closely aligned with the main direction of propagation of the Agulhas Current. Variations from the mean ASAR range velocities are plotted with a solid black line. The time series of ASAR range velocities show rapid and large fluctuations over periods of a few days and throughout the measurement period. Whether these high frequency fluctuations were real or due to "noise" cannot be tested due to the absence of in situ measurements in the region. The range velocities derived from the altimetry (AVISO) data set do not display high frequency modulations due to the temporal as well as spatial smoothing required to produce merged maps of geostrophic currents from sea surface height measurements.

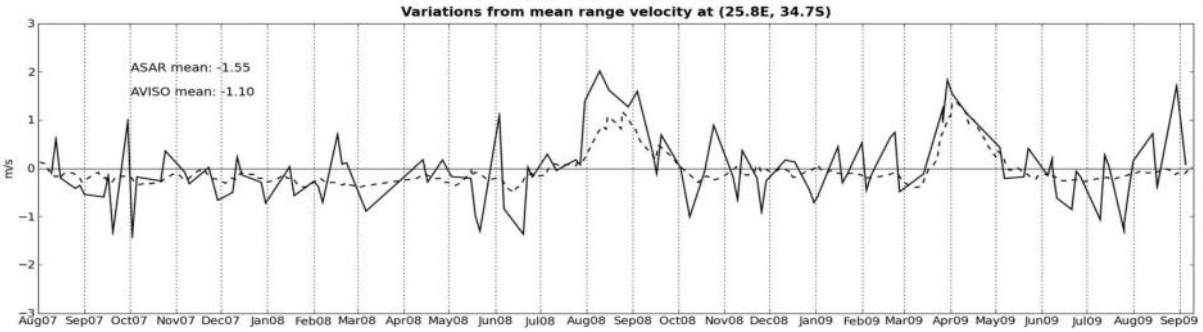

Figure 5: Fluctuations from the mean ASAR and AVISO range-directed surface current velocities (in m s−1) at the position of the mean local maxima in the Agulhas Current core, offshore Port Elizabeth (25.8°E, 34.7°S). ASAR range velocities are derived for all ascending path observations collected between August 2007 and September 2009 and are plotted as a solid black line. The range-directed surface current velocities projected for ascending path configurations and calculated by combining the CNES-CLS09 MDT with the AVISO NRT-MSLA daily product are plotted as a dashed line. The largest anomalies in the ASAR and AVISO range velocities were observed in August 2008 and April 2009 and were associated with the passage of Natal Pulses.

In conclusion, ASAR observations provide a direct measurement of the surface current velocity in the radar range direction while altimetry provides an indirect (geostrophy based) measurement of the surface flow. SAR and altimetry measurements differ significantly in their temporal and spatial coverage, while altimetry benefits from a better global coverage, geostrophic currents derived from altimetry can only be obtained along the altimeter track with repeat cycles varying between 10 and 35 days. ASAR measurements on the other hand are collected twice a day (ascending and descending orbits) but are spatially limited by comparison. Significant research efforts to improve wind retrieval algorithms from SAR are however still required to improve the quality of the range-directed surface velocities. Most importantly, for the Agulhas Current region, the SAR observations need to be validated against in situ observations.

2.2. Surface waves

Surface wave data is more complex than ocean currents which are simply measured in terms of velocity and direction of flow which vary with time. In contrast waves are random, quasi-regular and constantly changing with time. The wave field is made up of many waveforms each varying in amplitude, direction and superimposed. Hence wave characteristics and their prediction need to span three basic domains — time, f equency and probability. Their prediction can only be achieved through stochastic analysis using principle parameters such as the wave height, frequency and directional spectra. Associated with these are parameters such as the significant Wave Height (Hmo), mean 1/3 Wave Height (H3), maximum Wave Height (Hmax), Mean Period (Tm02), Peak Period (Tpeak), Mean Zero-Cross Period (z), Peak Direction (TpDir), Directional Spread (Spr1), Main Direction (Mdir), uni-directivity. Accurate measurement of the wave field is thus understandably challenging and has been attempted using a variety of techniques. Understanding the wave data and the limitations therefore requires knowledge of the various techniques.

2.2.1. Measurement techniques

Unlike ocean currents, a wide variety of techniques has been used to measure waves on the ocean's surface. Presently there are 5 main methods that can measure surface waves away from structures: (1) the surface wave rider buoy, (2) waves gauges (bottom-mounted water pressure sensor), (3) bottom-mounted Acoustic Doppler Current Profiler (ADCP), (4) land/platform based HF radar, and (5) satellite altimetry/radar.

In situ instrumentation

The first method – the surface wave rider bouy - uses an accelerometer mounted on a meteorological or other buoy type. The most accurate measurements are made using an accelerometer stabilized by a gyro so the axis of the accelerometer is always vertical. Double integration of vertical acceleration gives displacement. The double integration, however, amplifies low-frequency noise leading to the low frequency signals. In addition, the buoy's heave is not sensitive to wavelengths less than the buoy's diameter, and buoys only measure waves having wavelengths greater than the diameter of the buoy. Overall, careful measurements are accurate to 10% or better. The Datawell Waverider has become the standard, most reliable method of measuring surface waves and their direction. It measures wave height for wave periods of 1.6 – 30 s with an accuracy of 0.5% of the measured value.

The second measurement technique uses wave gauges mounted on platforms or on the seafloor in shallow water. Many different types of sensors are used to measure the height of the wave or subsurface pressure, which is related to wave-height. Sound, infrared beams, and radio waves can be used to determine the distance from the sensor to the sea surface, provided the sensor can be

mounted on a stable platform that does not interfere with the waves. Pressure gauges can be used to measure the depth from the sea surface to the gauge. Arrays of bottom-mounted pressure gauges are useful for determining wave directions and are widely used offshore of the surf zone to determine offshore wave directions. The pressure gauge must be located within a quarter of a wavelength of the surface because wave-induced pressure fluctuations decrease exponentially with depth. Thus, both gauges and pressure sensors are restricted to shallow water or to large platforms on the continental shelf. Similarly, accuracy is 10% or better.

The surface *Datawell waverider* buoy has for several years been the main method used to measure surface waves in the continual shelf (<100 m). However, their accuracy and precision has now been surpassed by the ADCP method (see Appendix B: Technical report on the *Performance of ADCP-Directional Wave Spectra and comparisons with other independent measurements*). As demonstrated in technical reports, the recently developed ADCP technique is now the preferred direct method of measurement in that it offers (1) accurate and well-resolved wave directional analysis similar to a spatial array of sensors, (2) direct measurement of surface variation like a surface-following device, (3) provides three independent methods of measurement simultaneously which are used to verify data quality (surface tracking, orbital velocity and pressure), (4) easy deployment of a bottom-mounted instrument at a single location, (5) safe from storms, shipping and instrument loss/theft, (6) measurements of surface-layer currents that distort the measured wave field (these data are internally used to correct the wave data), and (7) is cheaper than wave rider buoys.

Satellites

The launch of oceanographic satellites has provided a new and extensive set of data on the state of the ocean surface. These measurements are especially important for the study of deep oceans where reliable observations are almost non-existent. At present, in terms of ocean surface waves, the most important satellite remote sensing systems are SEASAT, GEOSAT, TOPEX-POSEIDON, RADARSAT, ERS-1 and ERS-2. An overview of all satellites deploying instruments detecting the ocean surface is given by Komen et al. (1994). There are three standard active microwave instruments of principal interest for surface wave detection — the altimeter, the Synthetic Aperture Radar (scatterometer. These instruments provide global, all weather, day and night data coverage. However, it is important to note that a typical polar orbiting satellite orbits the earth once every 100 minutes, which corresponds to a spacing of 2 800 km at the equator and a mean equatorial separation of all ascending and descending orbits within one day of 1 400 km. As the grid is filled in the spacing is reduced. For example GEOSAT was placed in a 17-day repeat pattern corresponding to ground track spacing of 163 km at the Equator and 82 km at a latitude of 60º. This data coverage is not sufficient for the computation of wind and wave fields on the typical synoptic scale of weather variability. Therefore, to interpolate the wind and wave fields in an optimal way, the data must be assimilated with available data from conventional observations or numerical models.

Satellite altimeters

The satellite altimeters used to measure surface geostrophic currents also measure wave-height. Altimeters were flown on SEASAT in 1978, GEOSAT from 1985 to 1988, ERS-1 & 2 from 1991, TOPEX-POSEIDON from 1992, and JASON from 2001. The technique uses a radio pulse from a satellite altimeter, which reflects first from the wave crests and later from the wave troughs. The reflection stretches the altimeter pulse in time and the stretching is measured and used to calculate wave-height. Accuracy is 10%. Altimeter data have been used to produce monthly mean maps of wave-heights and the variability of wave energy density in time and space. Altimeter observations are now being used with wave forecasting programs to increase the accuracy of wave forecasts.

Synthetic Aperture Radars on satellites

Synthetic Aperture Radars map the radar reflectivity of the sea surface with spatial resolution of 6-25 m. Maps of reflectivity often show wave-like features related to the real waves on the sea surface. The term "wave-like" is used because there is not an exact one-to-one relationship between wave-height and image density. Some waves are clearly mapped, others less so. The maps, however, can be used to obtain additional information about waves, especially the spatial distribution of wave directions in shallow water (Vesecky and Stewart 1982). Because directional information can be calculated directly from the radar data without the need to calculate an image (Hasselmann 1991), data from radars and altimeters on ERS-1 & 2 are being used to determine if the radar and altimeter observations can be used directly in wave forecast programs.

Wave data from satellites are gridded usually with a resolution of between 0.5 and 1.0º. Two commonly used data are AVISO Data and NCEP WAVEWATCH III Data:

- AVISO Data

The altimeter products are produced and distributed by AVISO (http://www.aviso.oceanobs.com/) as part of the Ssalto ground processing segment. These are merged and gridded data with a spatial resolution of 1° x 1° resolution. More information can be found at:

http://www.aviso.oceanobs.com/en/data/products/wind-waves-products/mswhmwind/processing-gridded-wind-wave-products.html.

The AVISO data are from the previous two days of each satellite observation. The data are processed and cross-calibrated using OSTM/Jason–2 as reference mission. First sigma0 and waves histograms are calibrated, and then the OSTM/Jason-2 wind algorithm is applied to cross-calibrated sigma0.

- NCEP WAVEWATCH III Data

Model data from NCEP WAVEWATCH III are hindcast reanalyses done by the Ifremer–IOWAGA with a 0.5° x 0.5° resolution. This data starts from 1994 and can be retrieved directly from the following addresses:

ftp://polar.ncep.noaa.gov/pub/waves/ and
ftp://ftp.ifremer.fr/ifremer/cersat/products/gridded/wavewatch3/HINDCAST/

2.2.2. History of wave recordings around the South African coast

The collection of wave data was initiated during the 1960's with a variety of instruments including clinometers, ship-borne wave recorders, pressure meters and inverted echo-sounders (Rossouw et al, 1999). During the 1970's a buoy, using an accelerometer, was introduced to measure waves at various locations along the coast. Since then, numerous wave buoys have been deployed, of which the Datawell Waverider buoy became the standard. Originally, non-directional buoys were used but since 2001 most of the buoys deployed around the coast measure the full directional wave energy spectrum. A full account of the development of wave measurements in South Africa can be found in Appendix B. Generally, wave data was collected on a project basis strongly driven and orientated around coastal engineering requirements.

However, with rapid development of South Africa's maritime sector, the need for real time wind and wave data increased and the recording of data had to be automated to provide an efficient and cost-

effective system. Authorities responsible for offshore structures (oil and gas installations such as the MossGas FA Platform) and the principal harbours of South Africa (the Transnet National Ports Authority) require detailed information on these wave fields so as to take appropriate action when extreme waves are expected. In particular, major ports in South Africa required real-time wave and wind data to improve ship operations. At the request of the Transnet National Ports Authority the *Integrated Port Operation Support System* (IPOSS) was introduced at all major ports shown in Figure 6 and is maintained by the CSIR. The development of this system also led to the establishment of the CSIR wave recording network, known as CSIR WaveNet, whereby a number of wave stations around the South African coast were positioned close to harbours and offshore structures, and are effectively managed and monitored. This remains the main source of measured wave data in South Africa.

2.2.3. CSIR WaveNet

The IPOSS systems located at each port constitute the coastal component of WaveNet. Each IPOSS system integrates data received from the wave buoy and the wind stations located near to each port (see Figure 6). The measured and predicted tide levels, as obtained from SANHO are also incorporated in IPOSS. Although all these systems are mainly operated for the National Ports Authority, useful information is also made available to the public and broader coastal community via the Wavenet website (http://wavenet.csir.co.za). The wind and wave information is graphically shown for all the measured locations. Whilst wave and wind measurements form the basis of the CSIR Coastal Systems, additional equipment is deployed and observations made to enhance the protection of particular ports. For example, an ADCP was deployed off Durban in 2002 and has been maintained to date.

a)

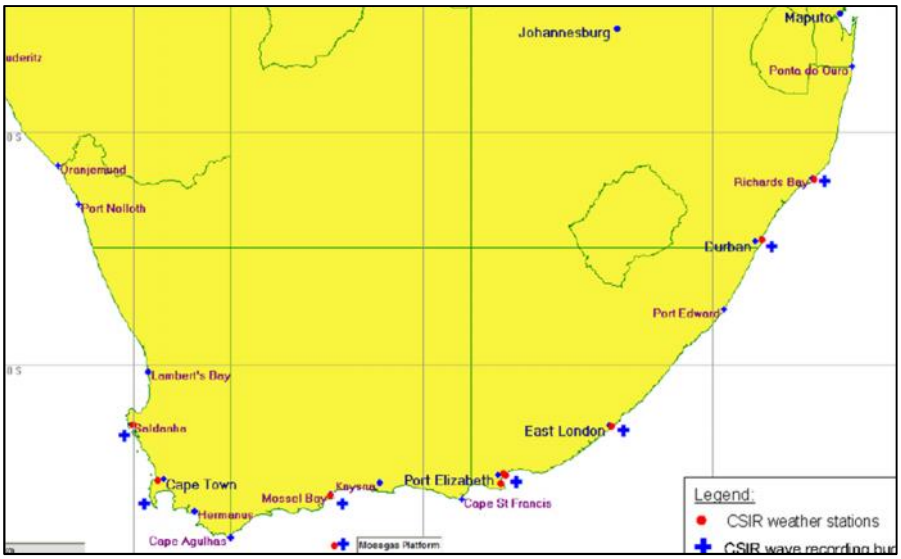

b)

CSIR Wave recording network

No	Location		Instrumentation	Approx. water depth	Deployment date
	Town	Description			
1	Saldanha Bay (West Coast)	Inside bay, approx. 1 km off Marcus Island	Non-directional Waverider buoy	23 m	Nov 1991
2	Slangkop (South-west coast)	Approx 6 km offshore of Kommetjie	Directional Waverider buoy	70 m	Jun 1994
3	Mossel Bay	Approx 3 km offshore of Hartenbos	Non-directional Waverider buoy	25 m	May 2007
4	Mossgas (FA) Platform	Approx 90 km South of Mossel Bay	Marex system	100 m	1996
5	Algoa Bay	Approx 3 km off Ngqura harbour	Directional Waverider buoy	20 m	Mar 2011
6	East London	Approx 1 km off harbour	Directional Waverider buoy	25 m	Apr 1992
7	Durban*	Approx 1 km off harbour	Directional Waverider buoy	30 m	Aug 2007
8	Richards Bay	Approx 2 km off harbour	Directional Waverider buoy	20 m	Nov 2002

**Note: the real-time ADCP current meter will also be re-deployed off the Port of Durban in the coming year.*

c)

Survey ID	Project Name	Survey/Station Name	Platform Name	Chief Scientist	Institute	Start	End	Stored?	Available?
2008/0543	Slangkop Waves		Waves	unknown	National Ports Authority (NPA)	1976-02-03	1993-06-12	Y	Y
2008/0541	Richards Bay Waves		Waves	unknown	National Ports Authority (NPA)	1979-01-02	1999-12-31	Y	Y
2008/0542	Saldanha Bay Waves		Waves	unknown	National Ports Authority (NPA)	1981-04-29	1999-12-31	Y	Y
2010/0008	East London Waves		Waves	unknown	National Ports Authority (NPA)	1992-04-22	1999-12-31	Y	Y
2010/0007	Cooper Light Waves		Waves	unknown	National Ports Authority (NPA)	1992-08-11	1999-12-31	Y	Y
2011/0005	Cape Point Waves		Waves	unknown	National Ports Authority (NPA)	1994-06-07	1999-12-31	Y	Y

Figure 6: (a) Map showing positions of the CSIR wave measurement stations located at major ports in South Africa. (b) Table provides the metadata for the 8 sites, (c) List of wave data available in the SADCO available to the public.

The locations of the wind and wave sites are depicted in Figure 6. Metadata pertaining to the sites are given in the table in Figure 6(c). Saldanha Bay and East London are the oldest sites established in 1991 and 1992 respectively, with Algoa Bay being the most recent addition in 2011. As shown in Figure 6(c) some data for six of these sites have been deposited in the SADCO data base but

inception dates of the times series do not correlate with those in Figure 6(b). All data from IPOSS are recorded by a private database at the CSIR which is available for research purposes only on request to SADCO who in turn facilitate the data retrieval. Originally the IPOSS data were collected on a 12-hourly basis but this has been increased to 6, 3, 1 and now 0.5 hours (Pers. Comm. Ursula von St Ange, SADCO).

2.2.4. Eskom Agulhas Bank wave studies

Eskom initiated a number of new wave measurements in 2011. The first of these comprised an inter-calibration experiment to assess the performance of various ADCPs on varying mooring lengths. These were compared with the Slangkop *IPOSS Datawell Directional II* buoy. This was followed by the deployment of long moorings mid shelf on the Agulhas bank between Slangkop and Cape Recife (typically in a depth of 80–120 m) and several coastal bottom-mounted moorings at 30 m. These studies are still in progress.

3. Ocean current resource assessment: Case study on the Agulhas Current

(Written by CRSES personnel Ms. I. Meyer & Mr. J. Reinecke)

The focus of this section of the report is to examine the available resource to extract energy from the ocean currents around South Africa. This section of the report examines all major aspects of the Agulhas Current, which includes the contributors to the Agulhas Current, the Agulhas Undercurrent and the variability of the current. The report evaluates this resource in respect to published data sets examining the capacity of the Agulhas Current. Stellenbosch University carried out a resources assessment by making use of the available data in order to draw conclusions about the feasibility of using the Agulhas Current as a sustainable, renewable energy resource.

3.1. The Agulhas Current

3.1.1. Macro effects

The largest source of water mass contribution to the Agulhas Current is the Agulhas Current retroflection. The continental shelf narrows between Durban and Port Edward causing the current to flow near the shore with a high velocity. The narrow shelf with a steep continental slope and uncomplicated topography helps stabilize the Agulhas Current in this region and thus no regular wide meanderings are present. There is one area of exception – The Natal Bight, situated between Durban and Richards Bay. This area has a wider continental shelf and the shelf's morphology change destabilizes the Agulhas Current, resulting in infrequent formation of Natal Pulses (Lutjeharms, 2006).

Other sources of water mass contribution are the strong Mozambique Current and the weaker East Madagascar Current. The contributions from these two sources are mostly in the form of eddies or rings.

3.1.2. Undercurrent

Another prominent feature of the Agulhas Current is the Agulhas Undercurrent. The presence of the Agulhas Undercurrent cannot be ignored when examining the overall transport and velocity profiles of the Agulhas Current. The undercurrent flows towards the equator along the continental shelf. The depth of the undercurrent varies with distance from shore but the undercurrent is found at deeper depths as the distance from the shore increases. Bryden et al (2005) states that the average depth of the undercurrent is 2 218 m in regions greater than 60 km from the shore.

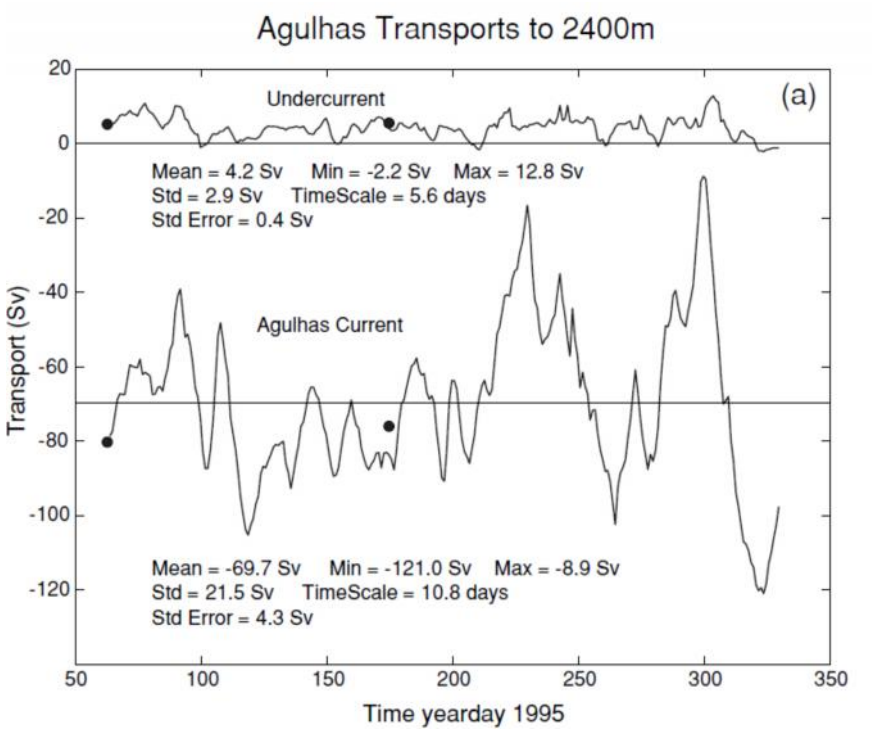

Figure 7: Agulhas Current transports (Bryden, et al., 2005)

The effects of the Agulhas Undercurrent can be seen in Figure 7 where a comparison can be made between the transport of the undercurrent and the Agulhas Current. It is seen that the Agulhas Current has a far larger transport capacity with large variability compared to the undercurrent's much smaller transport capacity but less variability. It has been calculated that the undercurrent transport is an average of 6±1 Sv (Beal & Bryden, 1999). This average in the North East direction shows that there is a persistent undercurrent. The Agulhas Current presents in a V-shaped profile, and the undercurrent always flanks this V-profile where one component runs alongside the continental slope and the other on the offshore side of the Agulhas Current V-profile (Beal, 2003). This formation is clearly seen in Figure 8 where the blue contours indicate the undercurrent. The presence of the undercurrent must be considered when examining the mooring depth and positions of components and overall transport values. However, it is seen that the Agulhas Undercurrent is relatively independent of the Agulhas Current for the undercurrent does not affect the velocity of the Agulhas Current (Bryden, et al., 2005). The undercurrent will affect power extraction technology performance if the technology is situated in the undercurrent's sphere of influence, due to the opposite direction in which the Agulhas Current and Undercurrent flow.

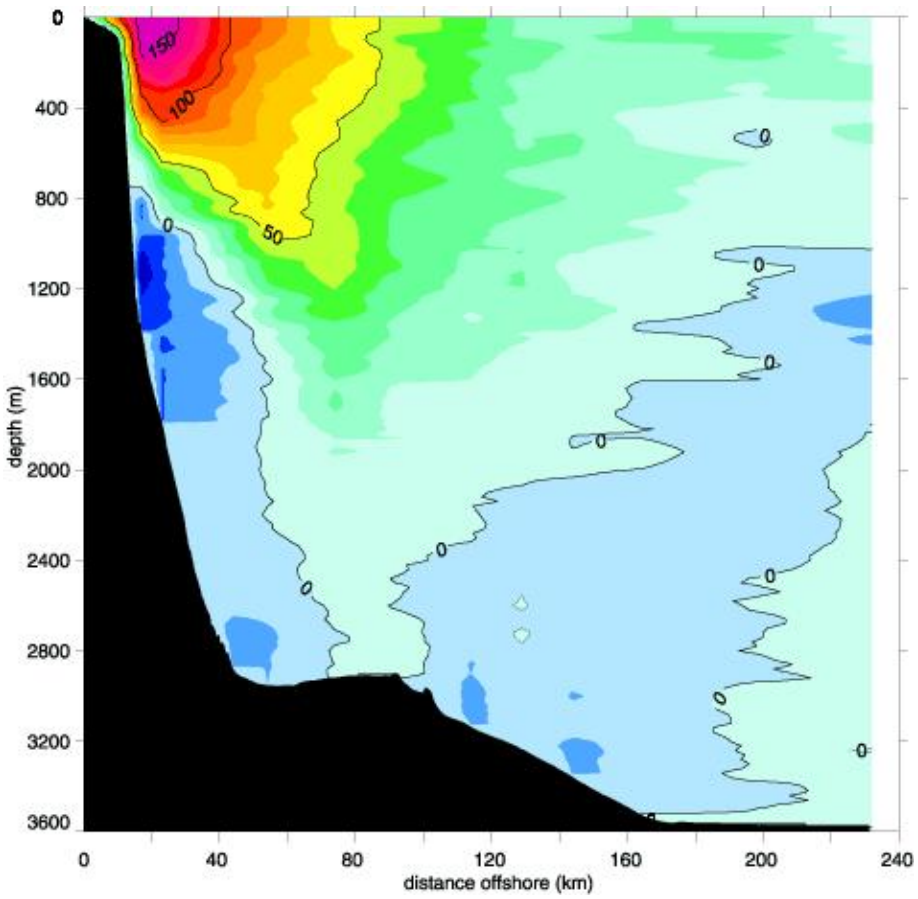

Figure 8: Position of Agulhas Undercurrent. The undercurrent can be seen in blue (indicating the negative flow direction) and the Agulhas Current in red (indicating the positive flow direction). The Agulhas Current flow indicated in red changes colour intensity for every 10 cm/s change in along-stream current (Beal, 2003).

With respect to calculating the overall available kinetic energy resource, both the Agulhas Undercurrent and Agulhas Current must be considered.

3.1.3. Variability

The variability is one of the main drawbacks of the Agulhas Current as a useful resource. These effects of the Agulhas Current variability must be carefully examined to help understand the nature of this resource. Variability is due to various factors. The dominant factor is the presence of the Natal Pulses, which form in the region of the Natal Bight (Rouault, 2011). Other factors include *forcing from external factors*, namely wind forcing from the Indian Anticyclone, and *forcing from source regions,* namely the Southern branch of the East Madagascar Current flowing through the Mozambique channel and recirculation of the Agulhas Current.

Natal Pulses

Natal Pulses are "large solitary meanders in the Agulhas Current associated with a cold-water core and a cyclonic circulation inshore of the current" (Rouault, 2011). The formation of the Natal Pulse is attributed to the change in slope of the continental shelf, which causes the instability of the current and the formation of these pulses. The pulses grow steadily in diameter as they move south-westward along the continental slope, with a typical diameter of 150 km (Rouault, 2011). The pulses have a phase velocity of approximately 10 to 20 km per day (Rouault, 2011). The pulses cause the Agulhas Current to move off course, so by the time the pulse passes the Port Elisabeth region, it has moved the Agulhas Current core approximately 200 km seaward of its normal location (Lutjeharms,

2006). It is found that Natal Pulses occur with a mean frequency of 4 to 6 times a year, with irregular time intervals of 50 to 240 days (Rouault, 2011).

The presence of a Natal Pulse is seen as the sharp decrease in velocity of the current close to the coast and the direction of the current reversing as the current passes over a specific point. The pulse can also cause upstream retroflection near Port Elizabeth and early shedding of Natal rings upsetting the normal flow regime. However, it has been found that the pulses are not present when the minima and maxima in transport are seen. Bryden et al (2005) noted that although weak transport is seen in the early stages of the Natal Pulse, near normal overall southward transport is experienced when the strongest cyclonic circulation is seen. The presence of the Natal Pulses in the Agulhas Current will impact the power extraction over an extended period of time as the presence of the Natal Pulse can reduce the velocity of the Agulhas Current to near zero and even reverse the direction of flow in an area. This phenomenon must be carefully analysed in order to determine the severity of the impact on the potential for resource extraction.

Seasonal variability and variability due to Neap and Spring tides

There has been no proof published in literature that there is seasonal variability or variability in the Agulhas Current due to Neap or Spring tides. More detailed research needs to be carried out for a long period of time to establish any annual or seasonal variability (Rouault, 2011).

With this basic understanding of the Agulhas Current the published data on the current can be analysed with insight into this resource.

3.2. Evaluation of published literature

In order to establish the validity of the published data, each published data set was evaluated and the findings are presented below. If the findings were found to be sound, they were incorporated into the resource assessment of the Agulhas Current.

In the article presented by Bryden, Beal, and Duncan, (2005) the structure, transport and temporal variability of the Agulhas Current was discussed. The Agulhas Current was measured with the use of 6 moorings perpendicular to the coast of Port Edward, as seen in Figure 9.

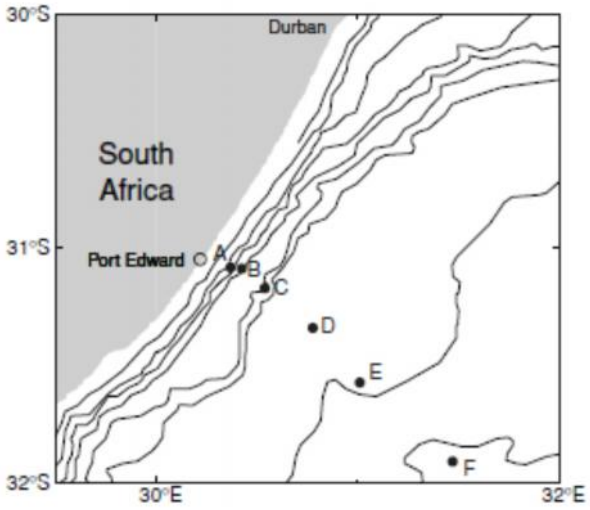

Figure 9: Mooring placement used by Bryden, Beal and Duncan (2005)

The six mooring were placed 13.4, 18.8, 32.4, 61.7, 101.9 and 152.8 km from the coast. With this placement of the ADCP (Acoustic Doppler Current Profiler) sensors, a full profile of the continental

shelf has been achieved. In order for a comprehensive representation of the behaviour of the Agulhas Current to be realised, the values obtained at specific depths at each of the mooring have been interpolated vertically and extrapolated laterally. This method of data manipulation has resulted in reliable values being achieved for the velocity of the Agulhas Current. Owing to the vast area that has been covered, the resolution of the data is coarse, where only daily values are taken from the temporal data. Bryden et al (2005) took the variability into account when examining the mean characteristics of the Agulhas Current through the use of composite spectral analysis. With the use of this analysis, the mean structure of the Agulhas Current has been developed as seen in Figure 10.

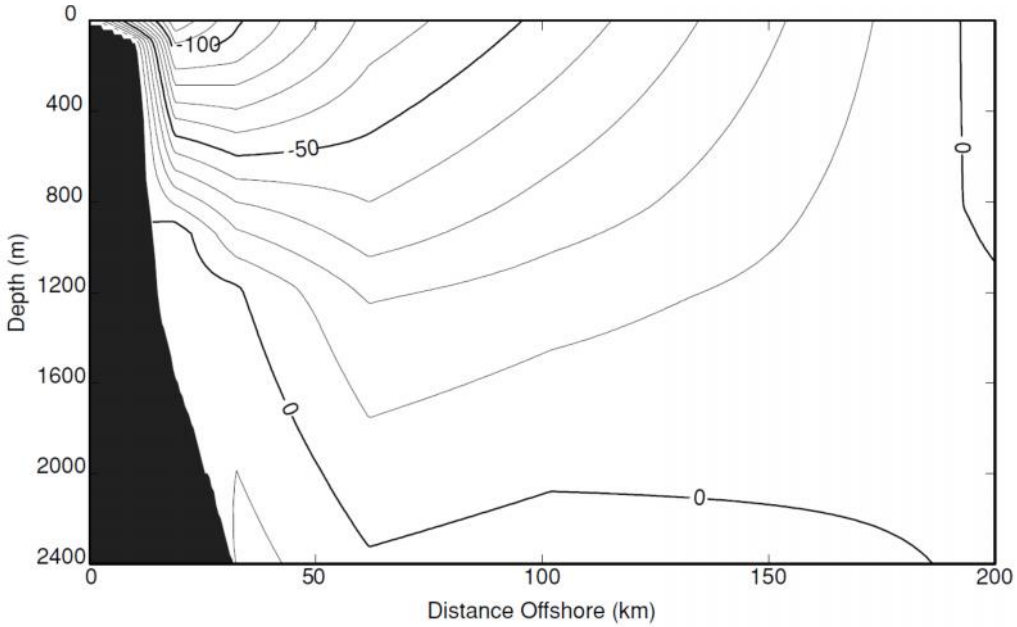

Figure 10: Mean structure of the Agulhas Current presented by Bryden et al (Bryden, et al., 2005)

Through the use of this mean structure, Bryden et al (2005) examined the total transport that is achieved by the Agulhas Current. Bryden et al (2005) also commented on the Agulhas Undercurrent and took this into consideration when determining the transport that is achieved by the current. It was concluded in the study that a transport of -69.7 Sv ± 4.3 Sv is achieved by the Agulhas Current at 31^{o} S, where the negative sign indicates the Southward direction in which the current flows.

In the report *The Velocity and Vorticity structure of the Agulhas Current at 32^{o}S* (Beal & Bryden, 1999), they presented further analysis of the Agulhas Current from an oceanography point of view. Again, in order to evaluate the current, 14 hydrographic stations were placed perpendicular to the coastline at a distance of 230 km from shore, as shown in Figure 11. Beal and Bryden (1999) considered salinity, density, oxygen level and temperature gradients as one indicator of the behaviour of the current. These measures indicate where Subtropical Surface Water, South Indian Centre Water, Red Sea Water and Antarctic Intermediate Waters lie and their associated behaviour.

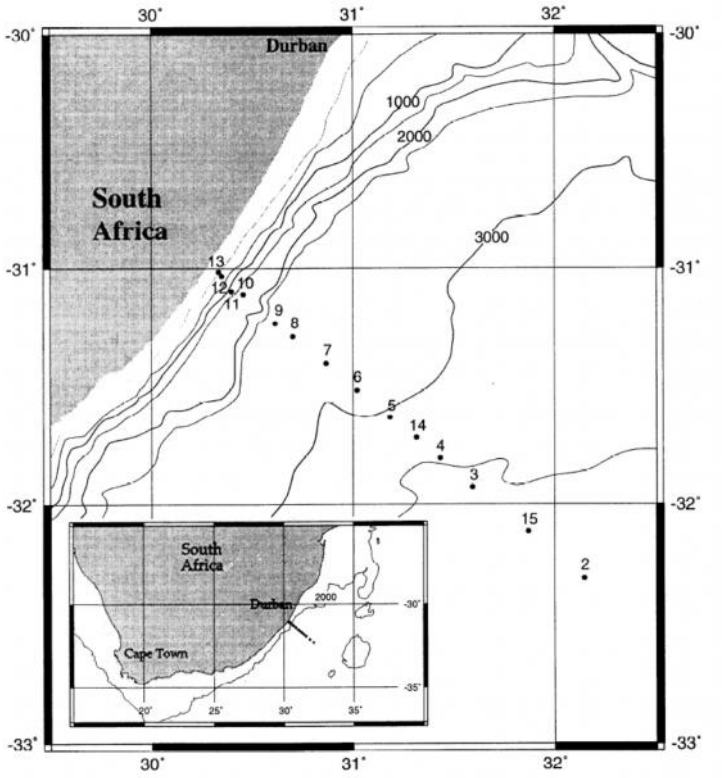

Figure 11: Hydrographic station placement (Beal & Bryden, 1999)

Beal and Bryden stated that the change in velocity structure of the current over large periods of time (years) is due to the density differences in the current. Beal and Bryden discovered that the core of the current is situated 20 km from the coastline at the surface and it is 70 km wide. The core of the current moves increasingly offshore with depth, this is seen in Figure 12. The report presented by Beal and Bryden was comprehensive in the data analysis and attempts to minimize the effects of velocity averaging when presenting the velocity profile of the Agulhas Current through the use of water mass considerations.

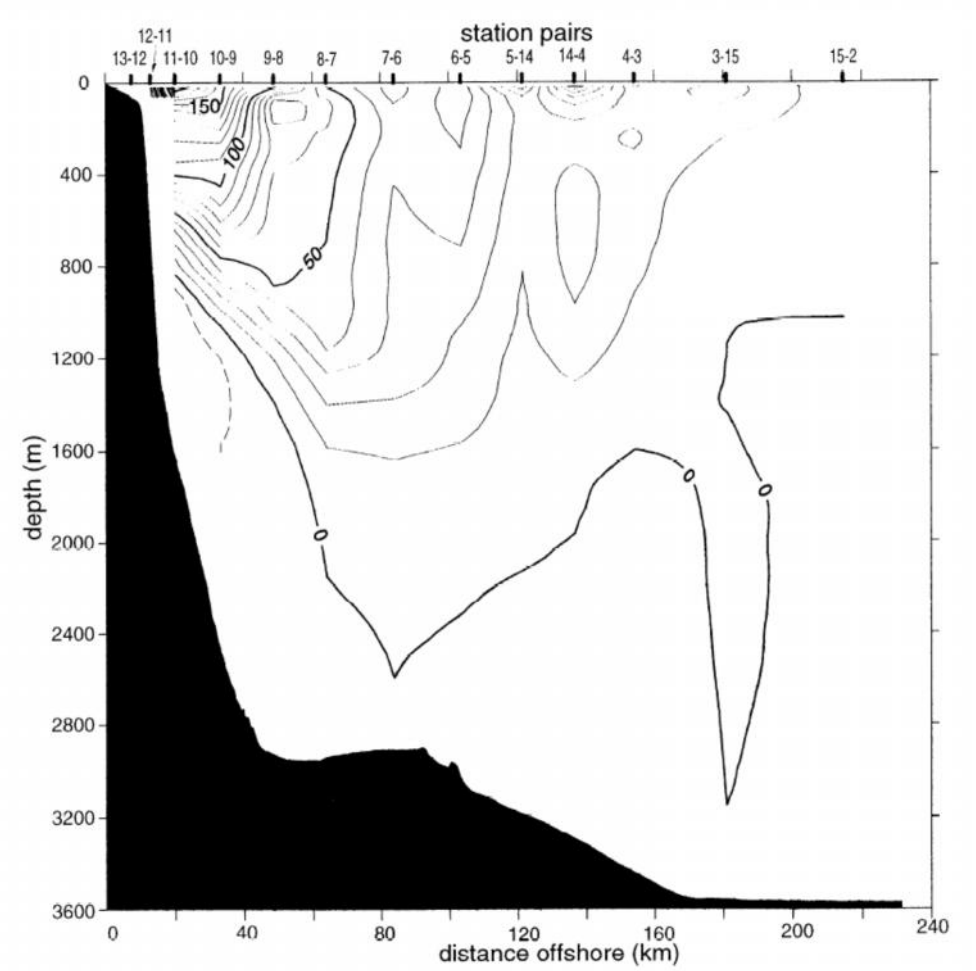

Figure 12: Velocity structure [cm/s] (Beal & Bryden, 1999)

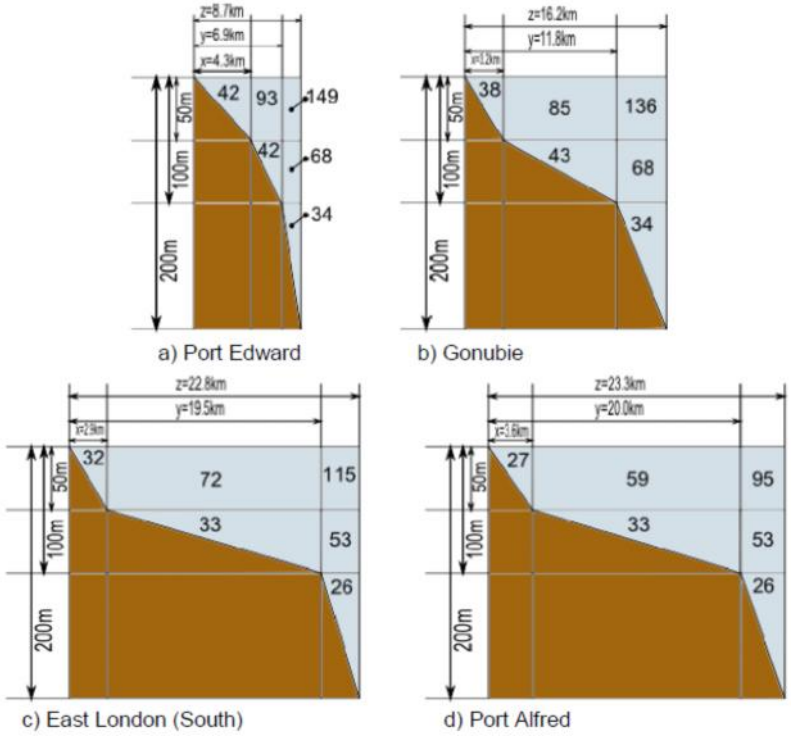

Figure 13: Velocity graphs presented by Moodley (R.Moodley, 2011) in [cm/s]

A report presented by Moodley (2001), focused on nearshore (less than 50 km from the coastline) assessment of the Agulhas Current. The integrity of the data presented is questionable as Moodley did not take the variability of the Agulhas Current into account and Moodley presented a very coarse area approximation of the Agulhas Current, shown in Figure 13.

In order to achieve the graphs presented in Figure 13, Moodley averaged the velocity values found in the available data. By doing this, the variability is not taken into account thus misleading conclusions can be drawn. By disregarding the variability, no change in direction of local velocity vectors were taken into consideration and the outliers present in the data set can skew the average value, again leading the reader to incorrect conclusions. There is no indication of a velocity gradient in Moodley's graphic approximation which further poses a problem when assessing the resource, for the core of the current cannot be seen and the effects of the undercurrent was ignored.

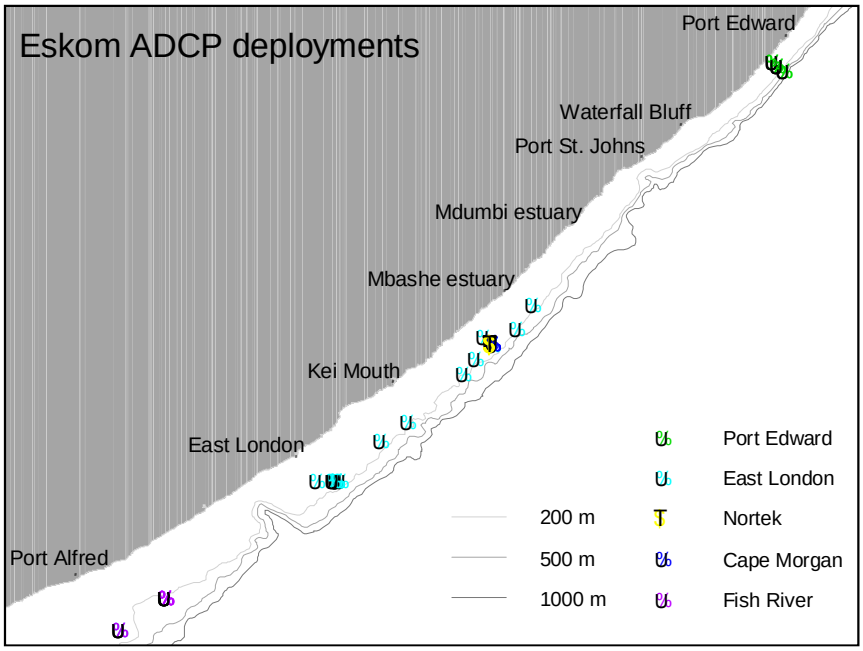

Figure 14: Locations of ADCP deployment

Another query to be raised about the graphs that Moodley presented is the integrity of the velocity versus the distance from shore information. Moodley plotted depth, distance and average velocity profile plots, which is questionable for the deployments of the ADCP's at differing locations were during different time periods, and not always at locations which could produce profile information. This leads to doubting the reliability of the data. Further, even if the different time periods are ignored, according to Figure 14 which shows the deployment of the ADCPs, the Port Edward site should be the only site which gives an indication of the distance from the shore in respect to depth and velocity. This is because inshore, mid-shelf and offshore measurements were taken with the perpendicular deployment of the ADCP's from the coast line. On further analysis of Figure 14 it is also seen that the East London deployment sites are scattered along the shelf but graphical data is presented as a single site by averaging the data of all the sites. This is a poor representation of the velocity of the Agulhas Current at this site. The data has also been collected by different types of ADCP instruments, which again questions the integrity of the data for no calibration data accompanies the analysis presented.

Making use of the same data set as Moodley, Elombo et al (2010) presented a more feasible analysis of the data. Elombo et al assessed the data by first finding the optimum depth of the current, and

finding the depth with the greatest velocity for each site. Then a temporal analysis was carried out at these depths in order to evaluate the variability of the current at that point. Elombo et al did not average the velocities over different time periods and over different locations, which establishes the validity of their analysis.

The study concluded that in respect to velocity magnitude, East London is the best site for harnessing the energy resource, and Fish River the worst. However the variation of the current is the largest at the East London site and smallest at the Fish River site. The operational depth is also of concern for the velocity of the current is greatly affected by the depth from the surface. It has been found that the MCT array will have to be placed 40 m from the ocean bed if the East London location is selected. This increases the difficulty of installation, as the closer to the ocean bed the easier the installation of the MCT. Elombo et al suggested the Cape Morgan site, due to its reasonable average velocity and feasible mooring depth of the MCT. They also stated that technology such as Minesto's deep green flying turbine should be further investigated and applied at sites which have the greatest velocity movement in the current, such as East London.

Rouault (2011) presented the report *Agulhas Current variability determined from space: a multi-sensor approach* (Rouault, 2011) and made use of Sea Surface Temperature (SST) data, surface current observations and Advanced Synthetic Aperture Radar (ASAR) technology in order to evaluate the Agulhas Current. The ASAR is the predominant source of data whereby the velocity of the sea surface is found by analysing the measured Doppler shift. This instrumentation is located on board the ENVISAT satellite of the European Space Agency (ESA). The ASAR is able to capture regions of strong current and shear and the high resolution at which it operates leads to minimal error. There is value in making use of remote sensing for the Agulhas Current has temperature differences, which indicate certain patterns and the surface height also varies with behaviour.

Remote sensing however only examines surface behaviour and traits and cannot be used to establish the characteristics of the current below the surface. It is these characteristics that are required when assessing a resource for marine current turbines. The surface speed of the Agulhas Current found using ASAR is seen in Figure 15.

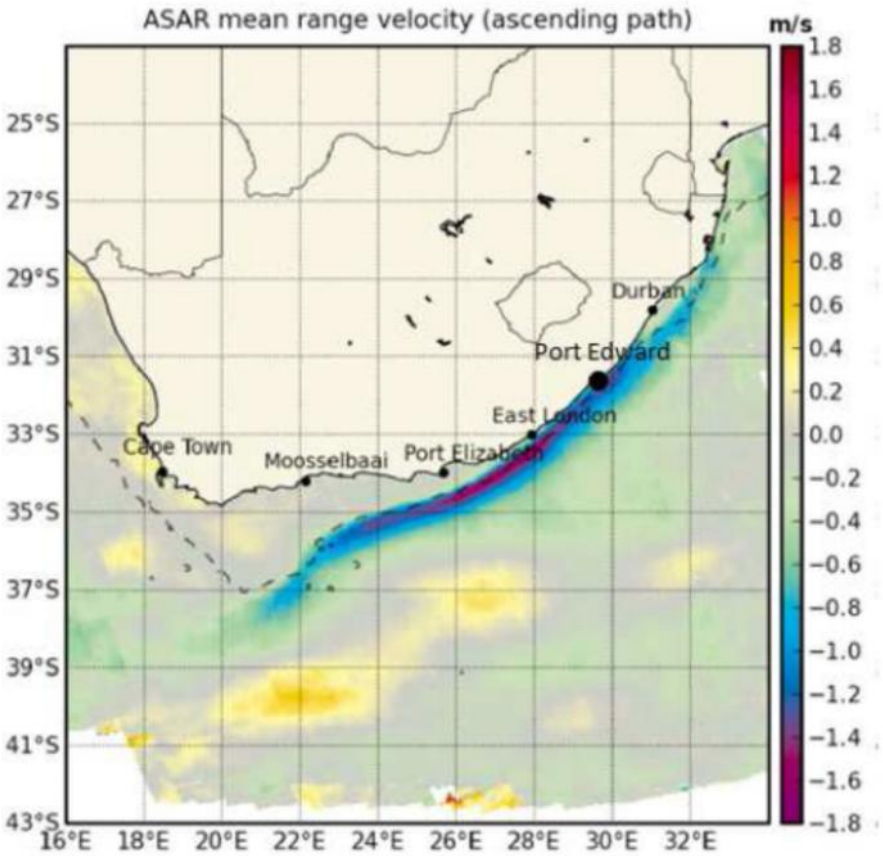

Figure 15: Surface speed of the Agulhas Current found using ASAR (Rouault, 2011)

3.3. Resource assessment

With the pitfalls identified in the published data and the understanding of the data presented, the resource assessment can be undertaken to determine the feasibility of installing marine turbines in the path of the Agulhas Current for power extraction. Table 3 shows a summary of the published data sets obtained through the use of ADCPs. Remote sensing data will be ignored during this analysis.

Table 3: Summary of published ADCP data sets

	Data set owners	Data set compilers	Time period of data collection	Range from shoreline	Resolution (number of ADCP moorings)
1	Data collected as part of World Ocean Circulation Experiment by Bryden, Beal and Duncan	Bryden, Beal and Duncan	March 1995 to April 1996	153 km	6
2	Agulhas Current Experiment	Bryden and Beal	February to March 1995	230 km	14
3	Public domain, originally owned by Eskom	Moodley, and Elombo et al	September 2005 to September 2010	Approx. 30km	51 (note: parallel not perpendicular to the coast)

3.3.1. The greater Agulhas Current

The results presented by Bryden et al (2005) and Bryden and Beal (1999) will be used to determine the overall power of the Agulhas Current. Table 4 shows a summary of the transport values found through the use of data set 1 and 2.

Table 4: Transport found in the Agulhas Current

	Data set compilers	Total poleward transport (Agulhas Current)	Total equatorward transport (Agulhas Undercurrent)
1	Bryden, Beal and Duncan	-69.7 ± 4.3 Sv	4.2 ± 0.4 Sv
2	Bryden and Beal	73 Sv	6 Sv

In order to make use of the published data sets 1 and 2, the conversion from Sverdrup to SI units needs to be stated:

$$Sv = 10^6 \ {}^{m^3}/_{s}$$

And it is known that instantaneous kinetic energy (power) is found by the following expression:

$$\dot{E_k} = \frac{1}{2}\dot{m}v^2$$

Where

$\dot{m}$ is the instantaneous mass flow rate
v is instantaneous current velocity

Since the measure of volume flow rate is known from the Sverdrup transport value, the mass flow rate of the Agulhas Current can be calculated and an average velocity can be deduced as follows:

$$\dot{m} = \dot{V} * \rho$$

Where $\rho \ is \ density = 1025 \ {}^{kg}/_{m^3}$

$\dot{V}$ is the volume flow rate
Thus velocity is calculated from:

$$v = \frac{Sverdrup \ transport}{Cross \ sectional \ area \ of \ Agulhas \ Current}$$

The total kinetic energy in the Agulhas Current will remain constant but the velocity will fluctuate as the bathymetry changes. This equation used to determine the kinetic energy of the Agulhas Current is a very rough estimate, but it will allow for an indication of the power contained in this body of water. Figure 16 and Figure 17 show where the area approximation has been taken for each data set. The area approximation aims to capture the area where the majority of the flow occurs.

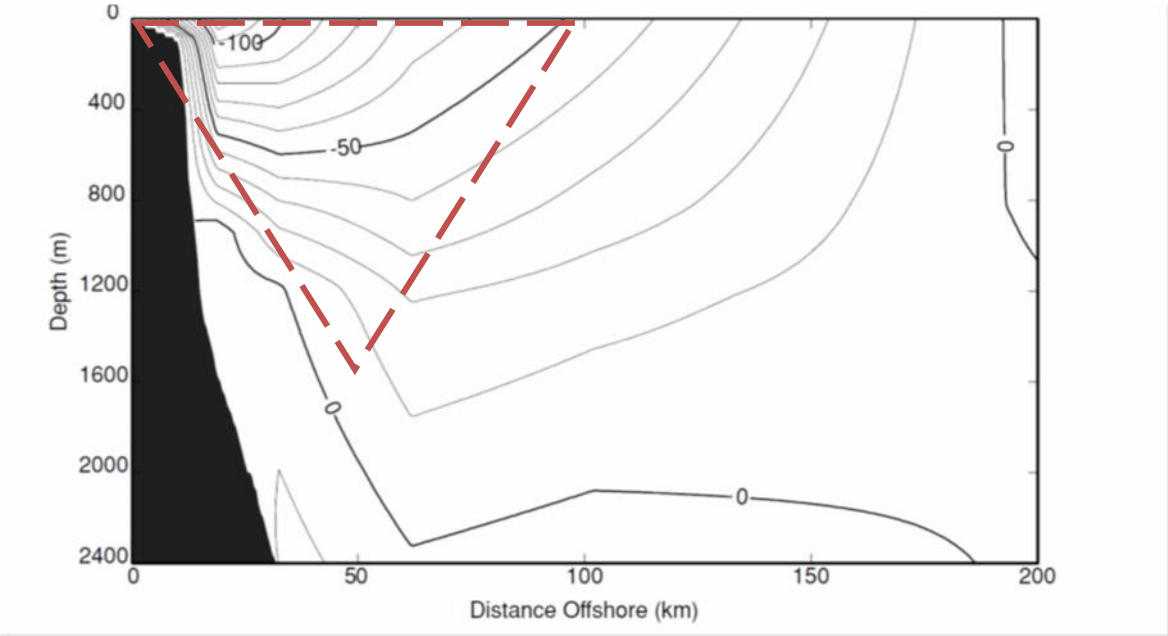

Figure 16: Area approximation for data set 1

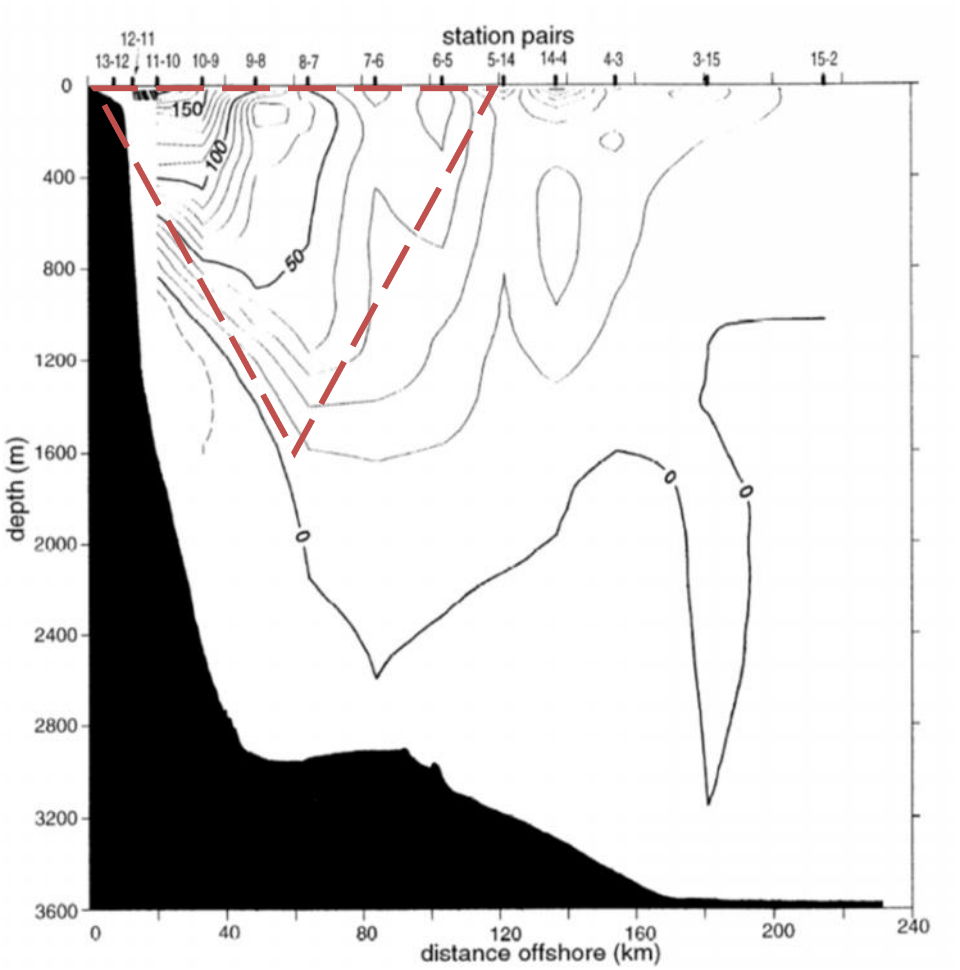

Figure 17: Area approximation for data set 2

Using these illustrations, the approximate area and approximate average velocity is found, in turn used to estimate the power of the current.

Table 5: Power contained in the greater Agulhas Current

	Data set compilers	Total poleward transport (Agulhas Current)	Approximate area over which transport was found	Approximate velocity	Power
1	Bryden, Beal and Duncan	-69.7 ± 4.3 Sv	190 km^2	0.87 m/s	27.1 GW
2	Bryden and Beal	-73 Sv	198 km^2	0.76 m/s	21.4 GW

The two power values calculated and shown in Table 5, lie within the same range of each other for such a basic approximate calculation. The power values are presented for an indication of the macro power of the Agulhas Current.

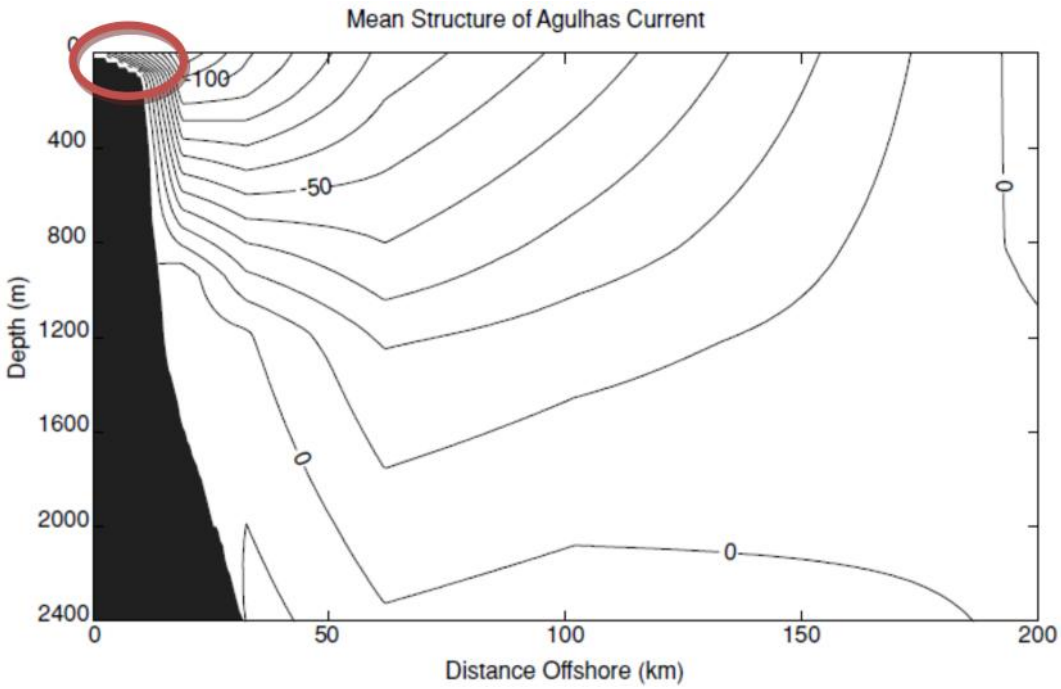

Figure 18: Area where depth constraint is satisfied (Bryden, et al., 2005)

The entire Agulhas Current has been evaluated above. The depth of the sea bed in most of the evaluated region is 2.4 km as seen in Figure 10 and Figure 12. However, most of the technology that is currently available for power extraction from ocean currents has been designed for tidal applications and thus operates at shallow depths of < 200 m. It is proposed that this technology be used for ocean current applications and thus sites of suitable mooring depth must be analysed. When analysing the cross section of the continental shelf, it is seen that there is an area in the profile where this depth constraint can be satisfied. This area is indicated by the red circle in Figure 18. The width of the continental shelf changes with location as is seen in Figure 19. The continental shelf just below Durban (30°S) is approximately 10 km wide and the shelf expands to 30 km at East London (33°S). It had been stated Bryden et al (2005) that the core of the Agulhas Current has been found at 31 km from the shore for 80% of the time measurements were taken at 31°S. Although this indicates that the area of highest velocity does not reside over the sites where there is suitable mooring depth, the velocity in the suitable mooring area will be analysed for the resource assessment.

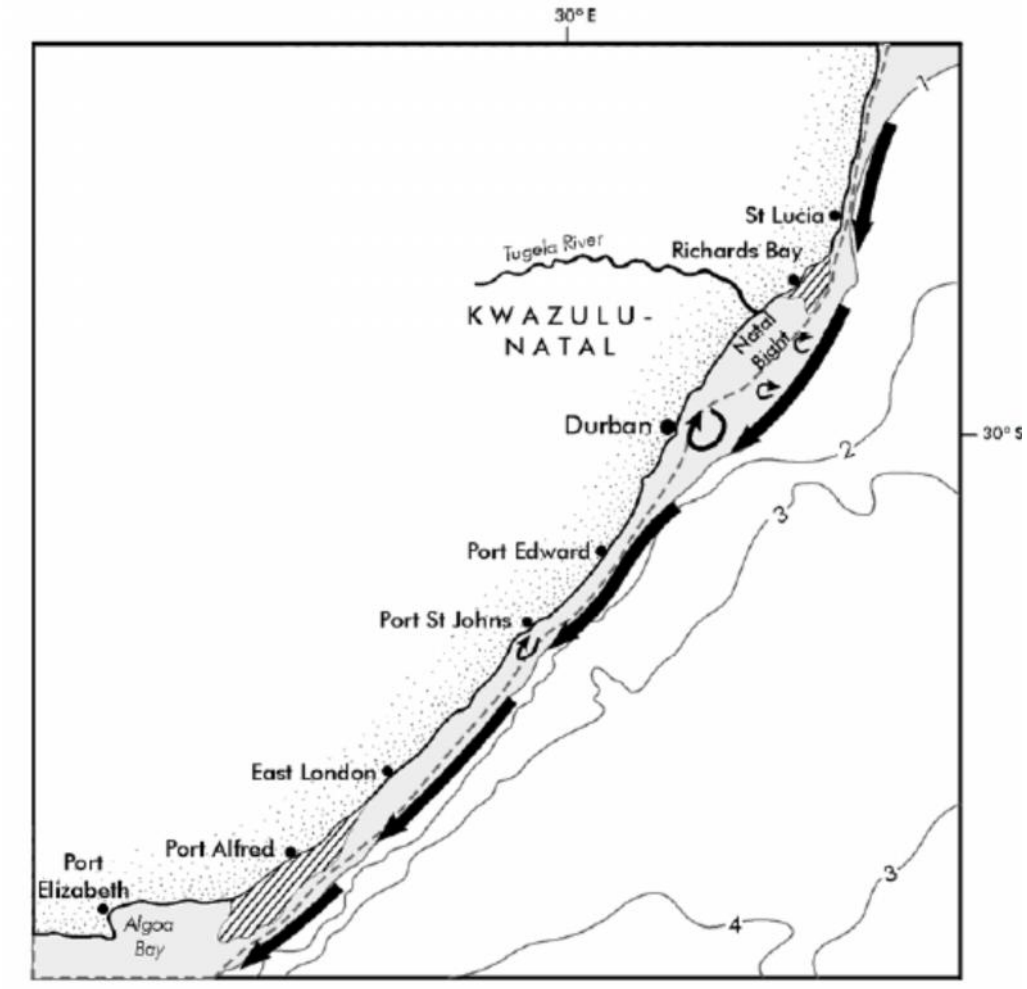

Figure 19: Bathymetry of the continental shelf along the northern Agulhas Current. The 200 m isobath is indicated by the dashed line and the continental shelf is shaded. (Simpson, 1974)

3.3.2. Focused assessment

The greater Agulhas Current has been examined but due to technology constraints, a focused assessment will be carried out on the areas with suitable mooring depth and available data. The data that was used for the focused assessment is the data available in the public domain supplied by Eskom.

Factors considered during assessment:

External factors that can impact the depth, location and available resource:

- *Shipping routes*: The presence of the Agulhas shipping route must be taken into consideration when analysing the resources for any technology installed for energy extraction. This technology must be located at least 20 m below the surface to allow sufficient clearance from the ship drafts.
- *Existing infrastructure that can utilize the generated energy*: the existing power grid will play a large role in determining the placement of the turbine farm.
- *Marine Protected Areas*: These areas cannot be used as suitable sites.

Technology specific factors:

- *Operational depth*: the operational depth of the technology is important to consider for this will limit the number of available sites that can be utilized.

- *Turbine Capacity factor:* Determines the practically extractable power
- *Array configuration and spacing:* Wake regions can affect extractable power down stream
- *Instrumentation used for data capturing:* Important to maintain the integrity of the data

The published raw data that is available lies within the required mooring depth. Figure 20 illustrates the data capture points. This data was used to analyse the Agulhas Current.

Figure 20: Points of available data

As already mentioned, when examining the current resource, it is important to also consider the site placement in respect to the established infrastructure to which the generated power can be connected. See Figure 21 for a map showing the main electricity grid of the Eastern Cape.

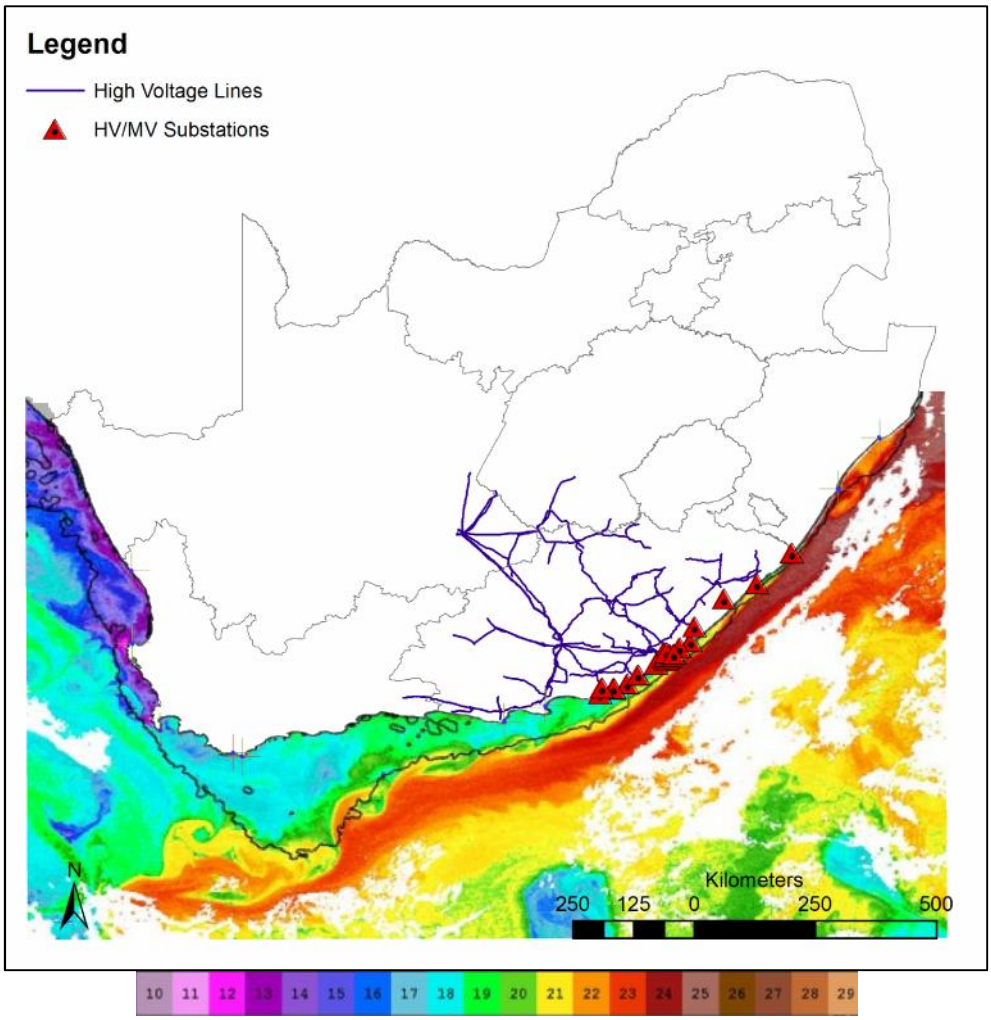

Figure 21: Illustration of the main electricity grid in the Eastern Cape

Figure 22 shows the proximity of the East London and Cape Morgan sites to the main grid. Figure 22 also shows protected marine areas that have to be taken into consideration when implementing the turbine farm.

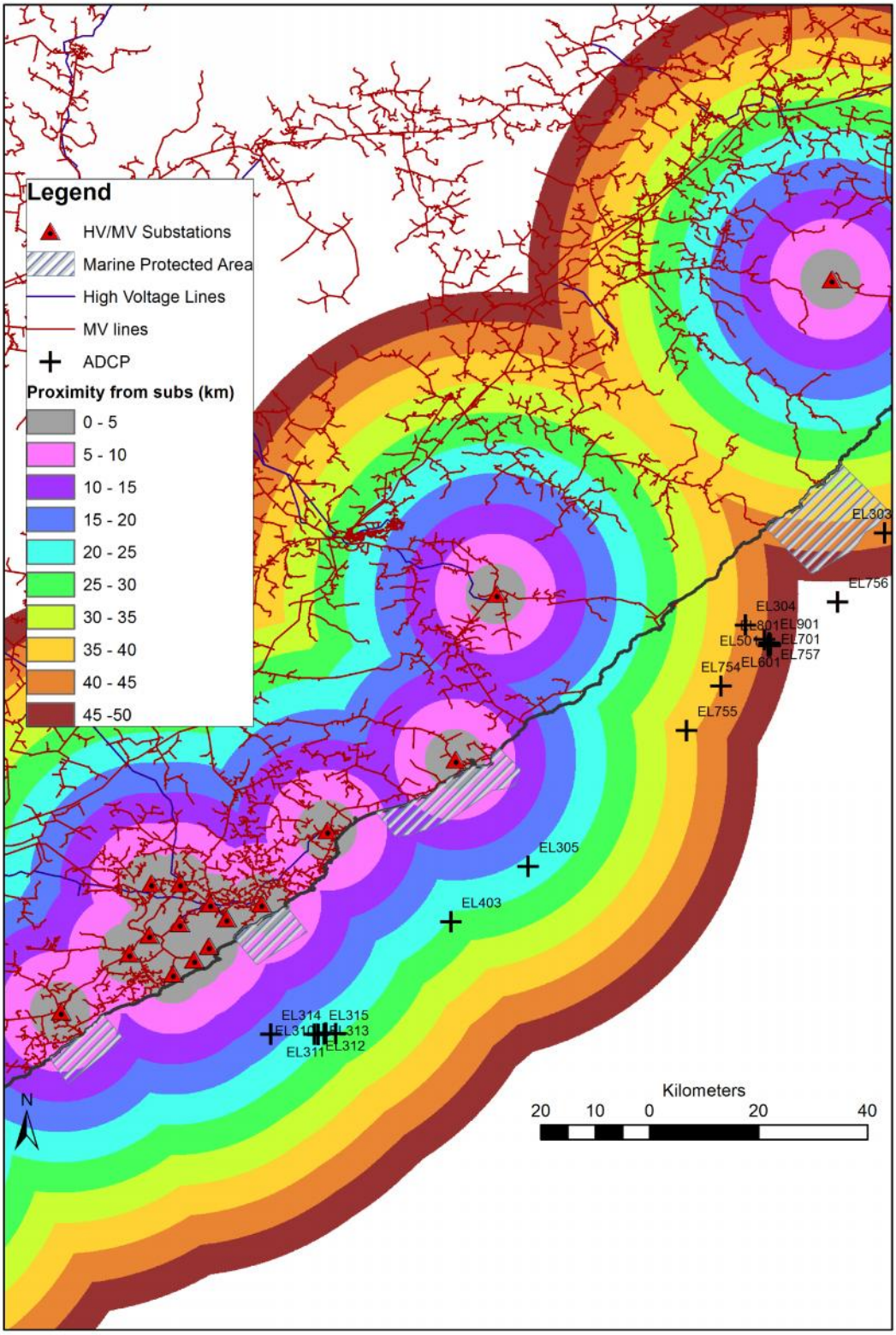

Figure 22: Illustration of all ADCP site deployments in relation to the substations and main grid connections

Bathymetry

Before assessment of the Agulhas Current can be carried out, it has to be determined whether or not the bathymetry of the continental shelf is important. During assessment of tidal resources, the shear stress imposed on the fluid flow by the boundaries of the channel is the main concern. However when considering the resource assessment of an ocean current, the boundaries of the channel are not going to impact the extractable resource as significantly as in the tidal application where the

effects of the channel need to be taken into consideration. The energy contained in the current lies in the upper portion of the water body rather than the deeper portion, hence the characteristics of Agulhas Current is analysed in this section. By analysing the current in the upper domain, the shear stress caused by the boundary between the ocean water and ocean bed can be ignored for it will have little impact on the upper portion of the water body.

In order to determine sites of promising capacity, first a basic analysis of the temporal velocity data obtained by each ADCP averaged over the time period is carried out. Then, when the promising sites have been determined, a full temporal analysis will be carried out.

3.3.3. Statistical analysis

The public domain data presented by Eskom has been used for the analysis. The details of the data can be found in Appendix A. The raw data that is useful is found in 3 to 5 month periods of ADCP deployment. Different ADCP types have been used at different sites, which will be noted where applicable. It must also be mentioned that consecutive deployments of ADCP's have not necessarily occurred at the same location, which can prove problematic when attempting annual analysis for one site. A note will be made at all sites where this poses a problem.

The tables below contain basic statistical analysis for each site at a depth of 20 m from the ocean surface. Figure 23 is a schematic of this explanation. Following this basic analysis, temporal velocity profiles will be presented for the best-identified sites.

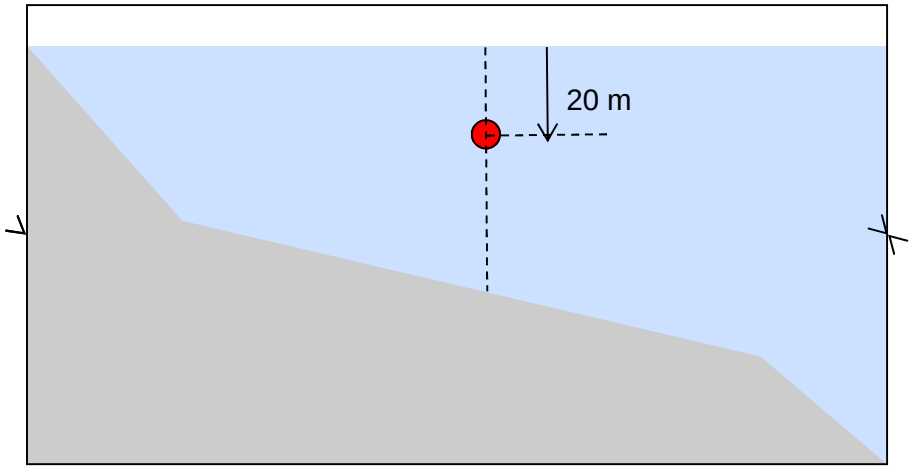

Figure 23: Schematic illustration of where the data measurements are taken (not to scale)

Table 6: Cape Morgan evaluation

		CM301 2008/07/12 -2008/12/13	CM302 2008/12/13 -2009/03/23	CM303 2009/03/23 -2009/08/25	CM304 2009/08/25 -2009/12/05	CM305 2009/12/05 -2010/03/03	CM306 2010/03/03 -2012/09/13
Sea bed depth		82.7 m	86 m	83.7 m	83 m	85.94 m	84 m
at 20 m depth	***Mean***	1.40	0.93	1.64	1.28	1.70	1.37
	Median	1.57	0.86	1.70	1.45	1.75	1.58
	Standard Deviation	0.60	0.63	0.48	0.52	0.48	0.65
	Kurtosis	-0.57	-0.94	0.26	-0.86	1.28	-0.73
	Skewness	-0.71	0.39	-0.67	-0.60	-0.93	-0.75
	Maximum	2.43	2.60	2.74	2.23	2.82	2.49

Table 7: Port Edward evaluation

		Midshelf			Offshore	
		PE301 2005/09/08 - 2005/12/11	PE302 2005/12/11 - 2006/04/10	PEM03 2006/04/10 - 2006/09/09	PE751 2005/09/08 - 2005/12/11	PE752 2005/12/11 - 2006/04/06
Sea bed depth		60 m	61.74 m	62.11 m	156 m	173.4 m
at 20 m depth	*Mean*	0.84	1.05	0.86	1.21	1.30
	Median	0.87	1.20	0.87	1.32	1.44
	Standard Deviation	0.36	0.44	0.36	0.56	0.57
	Kurtosis	-0.65	-0.52	-0.29	-0.86	-0.55
	Skewness	-0.23	-0.77	-0.04	-0.35	-0.69
	Maximum	1.80	1.92	1.92	2.38	2.38

Table 8: Fish River evaluation

		FR301 2007/08/18 - 2007/12/05	FR752 2007/12/08 - 2008/03/29	FR303 2008/04/01 - 2008/07/13	FR304 2008/07/13 - 2008/12/09	FR305 2008/12/12 - 2009/02/04	FR306 2009/03/21 - 2009/08/24	FR307 2009/08/26 - 2009/12/04	FR308 2009/12/04 - 2010/03/04	FR309 2010/03/04 - 2012/09/03
Sea bed depth		89.6 m	88 m	97 m	96 m	91.72 m	91.5 m	84 m	93. m	93.2 m
at 20 m depth	Mean	1.18	1.39	1.01	0.85	1.12	0.88	1.00	1.02	0.98
	Median	1.22	1.42	0.94	0.78	1.14	0.77	0.99	1.02	1.00
	Standard Deviation	0.48	0.51	0.59	0.51	0.54	0.55	0.50	0.55	0.58
	Kurtosis	-0.47	-0.72	-1.02	-0.06	-0.98	-0.68	-0.64	-0.82	-1.04
	Skewness	-0.22	-0.13	0.28	0.61	-0.12	0.50	0.20	0.13	0.18
	Maximum	2.48	2.73	2.44	2.67	2.19	2.55	2.44	2.77	2.33

Table 9: East London evaluation using the Nortek Sensor

Midshelf										
Nortek Sensor (Approx. location 1)										
		EL 1901	EL 201	EL 301	EL 401	EL 501	EL 601	EL 701	EL 801	EL 901	EL 1910
Sea bed depth		83.25 m	82.95 m	84.78 m	81.3 m	85.5 m	84.84 m	85 m	87 m	84.5 m	84.5 m
at 20 m depth	Mean	1.61	1.44	1.57	1.38	1.37	1.55	1.66	1.49	0.60	0.92
	Median	1.75	1.59	1.67	1.56	1.46	1.57	1.81	1.82	0.43	0.90
	Standard Deviation	0.50	0.54	0.47	0.59	0.57	0.31	0.55	0.76	0.50	0.60
	Kurtosis	1.18	-0.07	1.04	-0.88	-0.37	0.52	1.11	-1.30	0.32	-1.18
	Skewness	-1.26	-0.91	-1.01	-0.58	-0.46	-0.48	-1.29	-0.40	1.13	0.26
	Maximum	2.62	2.39	2.52	2.48	2.70	2.48	2.58	2.58	2.10	2.30

Table 10: East London evaluation using the RDI 75 Sensor

RDI 75 Sensor (location spread out)						
		EL403	EL754	EL755	EL756	EL757
Sea bed depth		96 m	91.99 m	102 m	196 m	83.86 m
at 20 m depth	Mean	1.23	1.51	1.43	1.48	1.78
	Median	1.33	1.61	1.63	1.56	1.79
	Standard Deviation	0.54	0.48	0.61	0.59	0.33
	Kurtosis	-0.76	0.72	-0.73	0.08	0.32
	Skewness	-0.49	-0.95	-0.65	-0.52	-0.43
	Maximum	2.31	2.48	2.60	3.22	2.73

Table 11: East London evaluation using the RDI 300

RDI 300 Sensor (Approx. location 2, some outliers present)														
		EL 303	EL 304	EL 305	EL 306	EL 307	EL 308	EL 309	EL 310	EL 311	EL 312	EL 313	EL 314	EL 315
Sea bed depth		96 m	90 m	88.8 m	98.7 m	83.5 m	85 m	88.7 m	82 m	83.1 m	86 m	82.7 m	89.0 m	88 m
at 20 m depth	Mean	1.41	1.11	1.48	1.38	1.58	1.84	1.36	0.88	1.22	1.39	1.19	1.30	1.16
	Median	1.53	1.16	1.67	1.54	1.63	1.88	1.57	0.83	1.42	1.48	1.20	1.45	1.31
	Standard Deviation	0.55	0.45	0.62	0.65	0.44	0.38	0.75	0.51	0.72	0.51	0.51	0.59	0.69
	Kurtosis	-0.24	-0.51	-0.40	-0.93	0.21	-0.20	-1.22	-0.92	-1.30	-0.60	-0.89	-0.60	-1.28
	Skewness	-0.75	-0.33	-0.80	-0.50	-0.61	-0.43	-0.34	0.25	-0.32	-0.56	-0.05	-0.65	-0.10
	Maximum	2.58	2.13	2.73	2.58	2.83	2.78	2.75	2.22	2.62	2.37	2.30	2.67	2.79

In tables 6 to 11, it is seen that some values have been highlighted. These values are where a mean velocity of greater than 1.2 m/s has been observed. A mean value of 1.2 m/s has been chosen, for this indicates that the current will flow at speeds applicable for marine turbines for a large portion of the operating time. This will be confirmed later with capacity factor analysis. When examining the values achieved from the statistical analysis, it is seen that Cape Morgan and East London locations prove to be the most promising sites (Table 6, Table 9, Table 10, and Table 11). The position of these two locations can be seen in Figure 24. It is seen that the location East London 2 will be the better choice in respect to proximity to the nearest substation. Figure 24 also shows protected marine areas, which have to be taken into consideration when implementing the turbine farm. These areas should not pose a problem, as the direct lines from both chosen sites do not run through the protected areas.

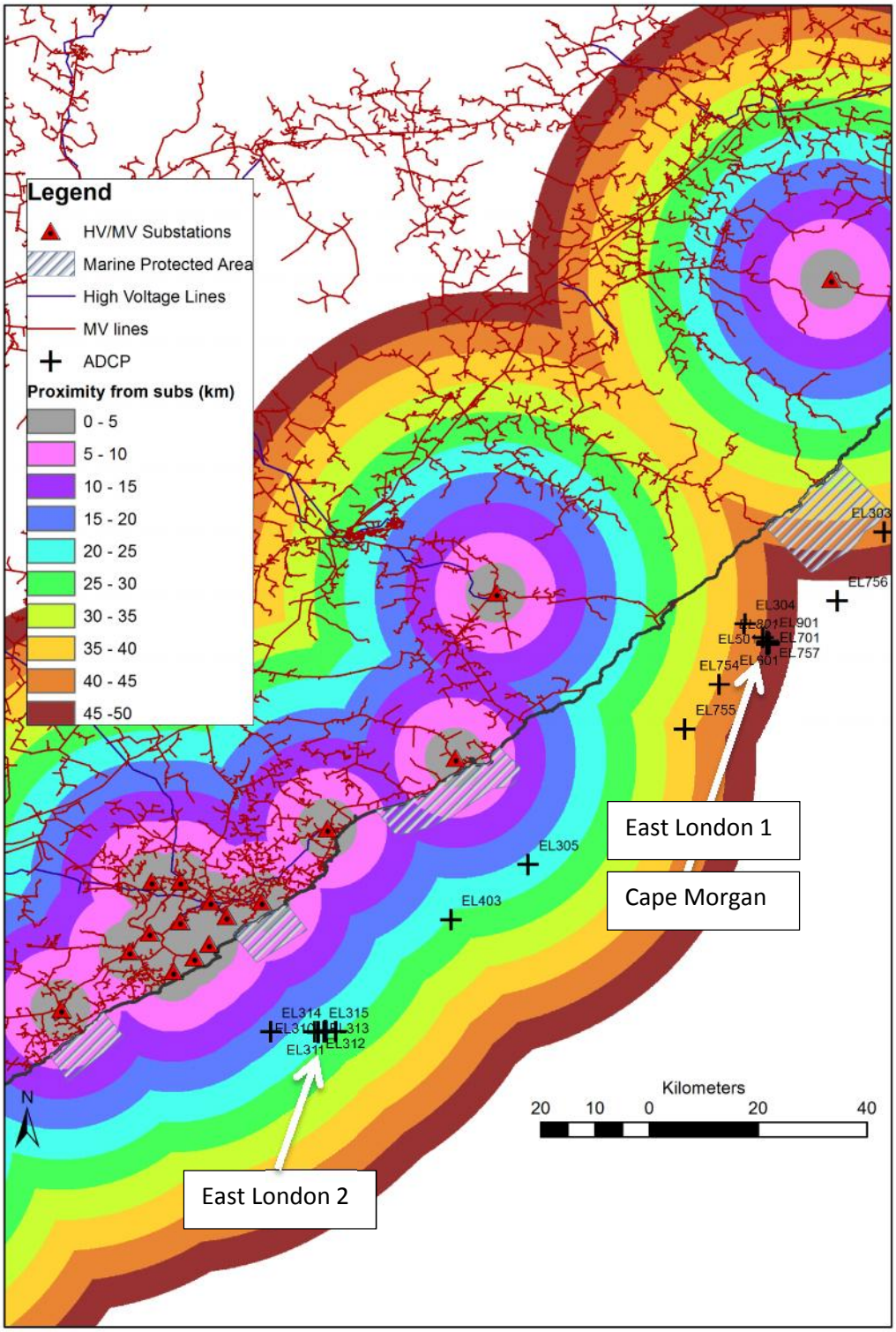

Figure 24: The two promising locations are shown with respect to the substations and electricity grid

Table 12 shows the data sets which will be further analysed in a temporal analysis. The data sets which have been chosen are the longest consecutive sets of data available obtained by the same type of ADCP at the same location. None of the data sets have the same time period but since all the time periods are longer than a year these data sets are assumed indicative of the behaviour of the current at the selected locations.

Table 12: Summary of data analysed

Data set	Location	ADCP type	Time period
Cape Morgan	-32.507 S 28.831 E	RDI 300	2009/03/23 to 2010/09/14
East London Location 1	-32.507 S 28.831 E	Nortek	2006/04/11 to 2008/04/30
East London Location 2	-33.150 S 28.099 E	RDI 300	2007/08/18 to 2009/03/22

3.3.4. Variability

A temporal analysis has to be carried out in the selected areas to investigate the current variability. As mentioned in section 3.1.3 of the report, the predominant mode of variability of the Agulhas Current is the presence of the Natal Pulses. Standard deviation of the site at 20m depth can be seen in the above tables. The following graphs present temporal plots of the annual current behaviour which illustrates the presence of the Natal Pulses. Each of the three sites will be addressed separately.

Cape Morgan

In order to determine the variability in the Cape Morgan area, there are 4 ADCP's, CM303 to CM306 which have been placed consecutively after each other within 100 m of desired location. This 100 m difference is an acceptable error for the bathymetry does not change over this area. This leads to an approximate 18 month period of consecutive data which can be analysed. The data set starts on 2009/03/23 and runs to 2010/09/14 and the data is analysed at a depth of 20 m. Table 13 shows the standard deviation which is a good indicator of variation of the velocity in the current.

Table 13: Cape Morgan 18-month data analysis

Mean [m/s]	1.46
Median [m/s]	1.6
Mode [m/s]	1.76
Standard Deviation [m/s]	0.59
Minimum [m/s]	0
Maximum [m/s]	2.82

When examining the temporal plot, Figure 25, in the 18 month period which has been presented, the presence of three Natal Pulses can be seen. The presence of the Natal Pulses is identified through the 20-day period of low velocity and in Figure 26 the change in direction can be seen when the Natal Pulses occur. The presence of smaller eddies can be seen by the change in direction for approximately 1 day periods in Figure 26. Another feature notable in Figure 25 and Figure 26 is the change in data behaviour around the data of 01/12/2009. There is a shift in the average direction of the current flow at this point. Also, the velocity becomes less variable and only large fluctuations occur when the Natal Pulses pass the measuring point. This could indicate an instrumentation flaw of incorrect calibration and drift readings, and must be considered when final conclusions are being made about this data.

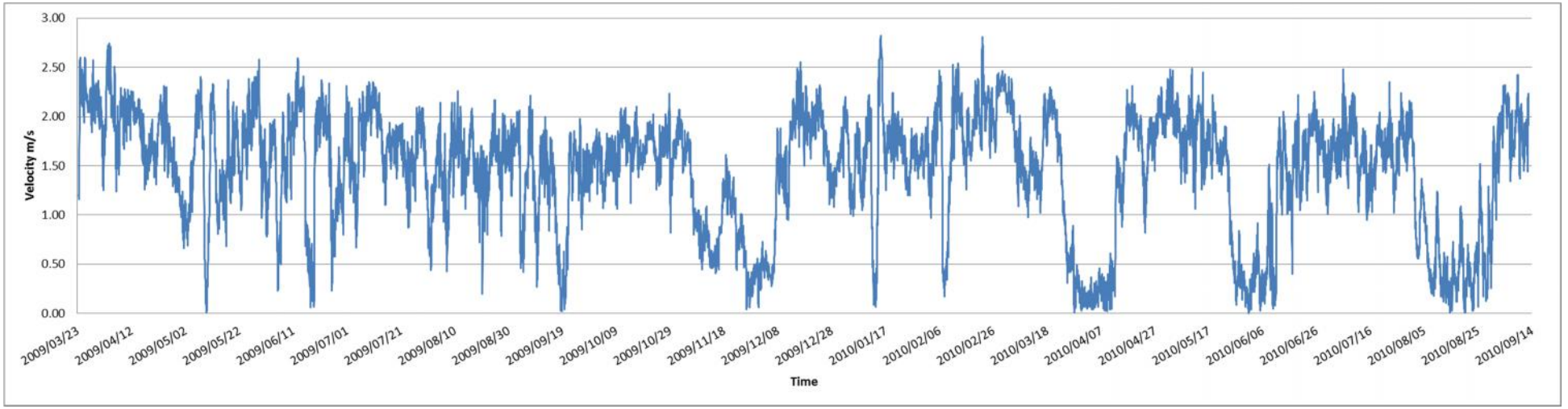

Figure 25: 18 month temporal velocity plot for Cape Morgan

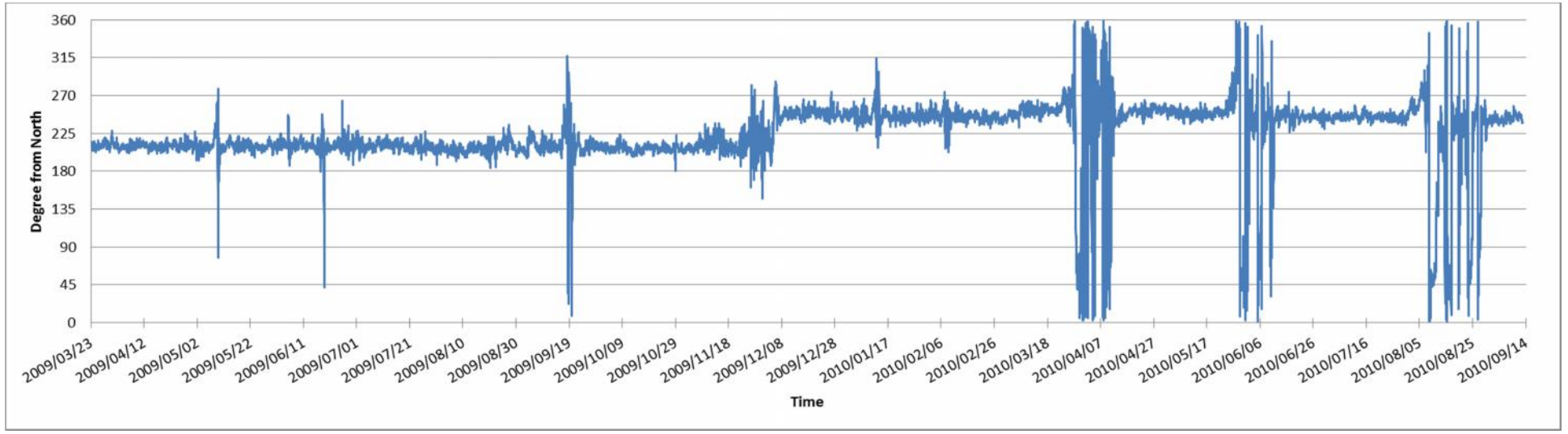

Figure 26: 18 month temporal directional plot for Cape Morgan

Another measure of variability that will help formalise the flow characteristics is a probability of exceedance plot. The plot for Cape Morgan can be seen in Figure 27. A summary of the findings of this plot can be seen in Table 14.

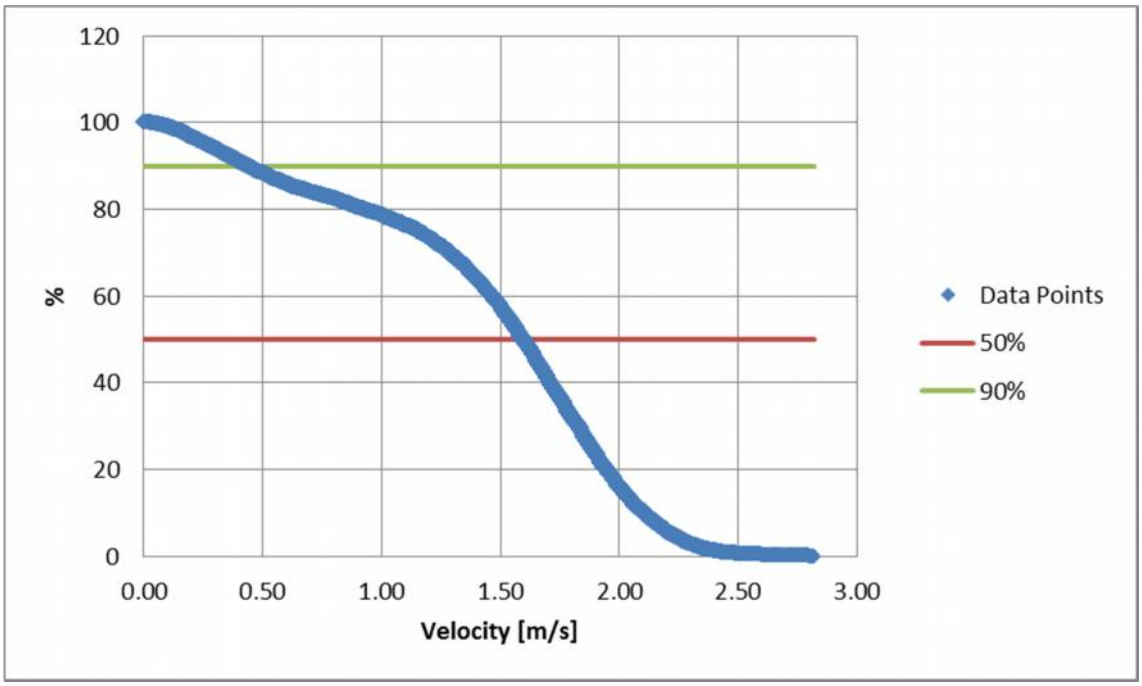

Figure 27: Exceedance of probability plot for Cape Morgan

Table 14: Summary of probability of exceedance for Cape Morgan

Probability of exceedance	Velocity [m/s]
P50	1.6
P75	1.15
P90	0.44
P99	0.1

Figure 28 and Figure 29 show a histogram of the data and the normal distribution plot of the velocity data. The two distinct peaks in the histogram curve show the predominance of the low velocity data. It is seen that the normal distribution plot is skewed slightly to the left, again reiterating the presence of low velocity occurrence. The wide bell observed in Figure 29 indicates the large variability of the current as there is a large distribution of the velocities, which have been recorded for the Agulhas Current. This trend is seen in the following figures when the normal distribution is evaluated for a site.

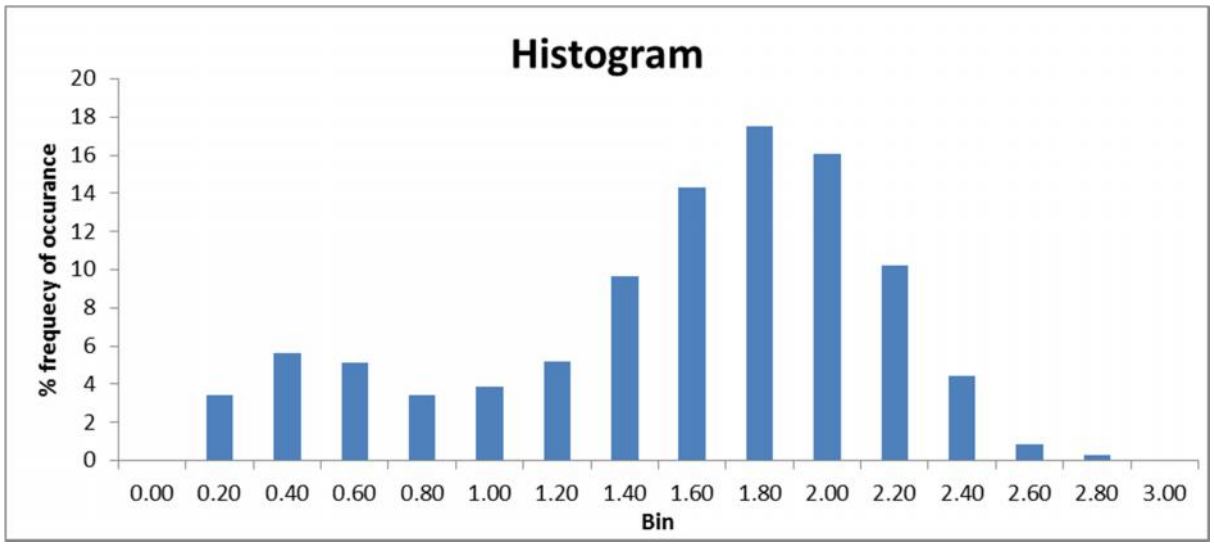

Figure 28: Histogram of velocity data

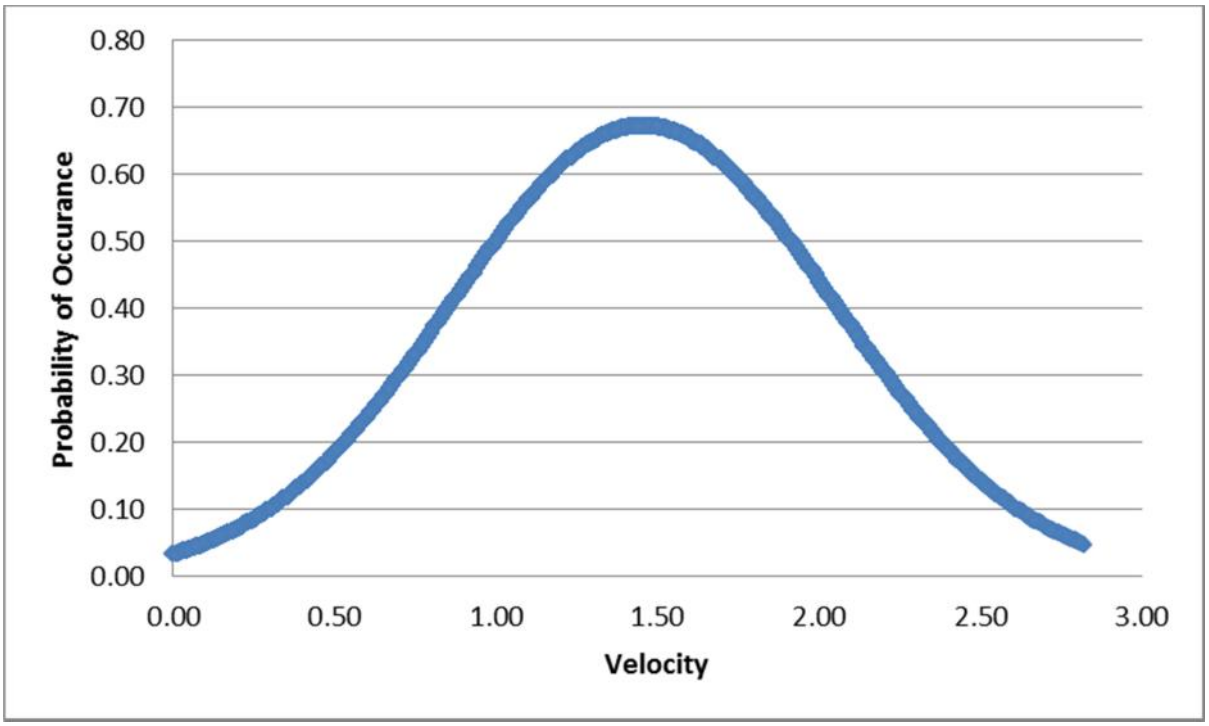

Figure 29: Normal distribution curve of velocity data

East London

There are two distinct locations where the majority of the ADCP's have been deployed for the East London area; these locations are seen in Figure 30. It is noted that the Cape Morgan data analysed was also captured at location 1, illustrated in Figure 24.

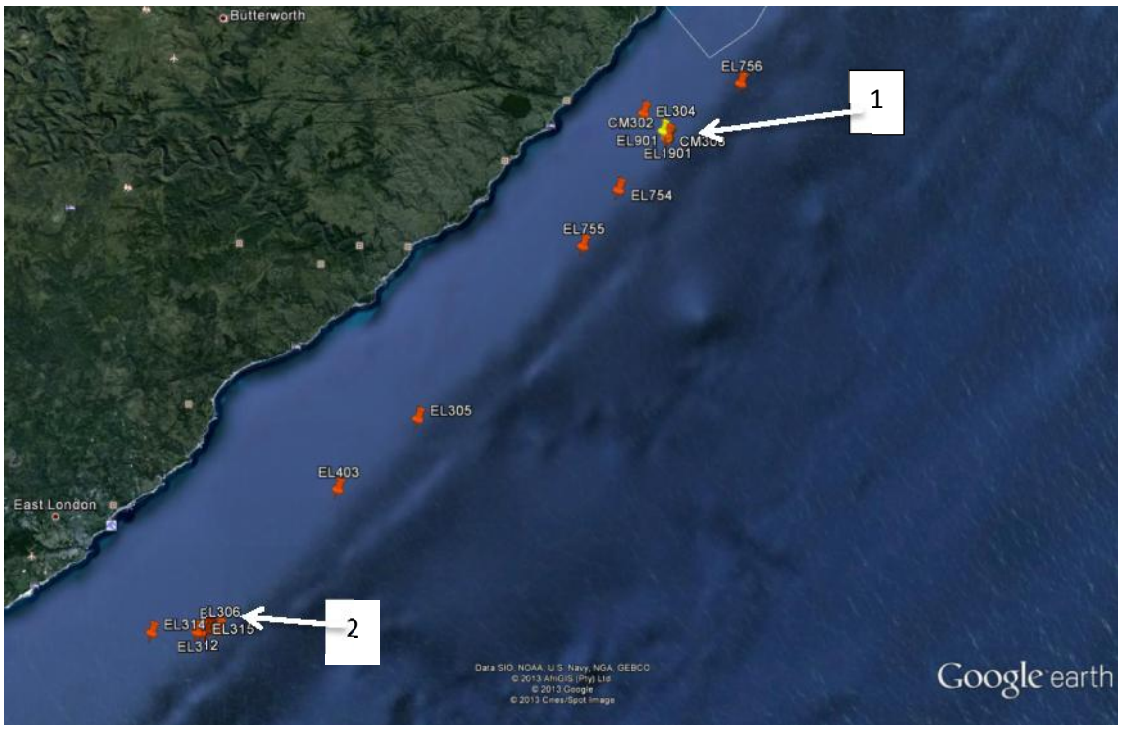

Figure 30: ADCP deployment locations for the East London Site

There is a 24 month consecutive data range available for site 1 with the ADCP deployments being within 100 m of each other. The same type of ADCP was used for each deployment and hence the data set has a continued integrity. The data set runs from 2006/04/11 to 2008/04/30. Table 15 shows the standard deviation of the 24 month data set. Figure 31 and Figure 32 show the temporal analysis for East London location 1.

Table 15: East London location 1

Mean [m/s]	1.48
Median [m/s]	1.59
Mode [m/s]	1.44
Standard Deviation [m/s]	0.53
Minimum [m/s]	0.009
Maximum [m/s]	2.7

It is interesting to note the difference in the recorded behaviour of the Agulhas Current at this location during the two different time periods, the one being that of the Cape Morgan site (analysed above) and the other the East London location 1. It is seen in Figure 31 and Figure 32 that there are two occasions where the velocity drops significantly and the direction changes, these instances can be seen at 2006/05/11 and at 2007/06/05. This drop in velocity and change in direction alludes to the presence of Natal Pulses. In this two year period that is analysed, only two, Natal Pulses are seen. Whereas in the 18 month period analysed from 2009/03/23 to 2010/09/14 there are three Natal Pulses which significantly impact the variability analysis. This also highlights the irregularity and unpredictable nature of this phenomenon. It is important to note that the standard deviation and mean is very similar for both time periods at this location indicating the continuity and integrity of the analysis.

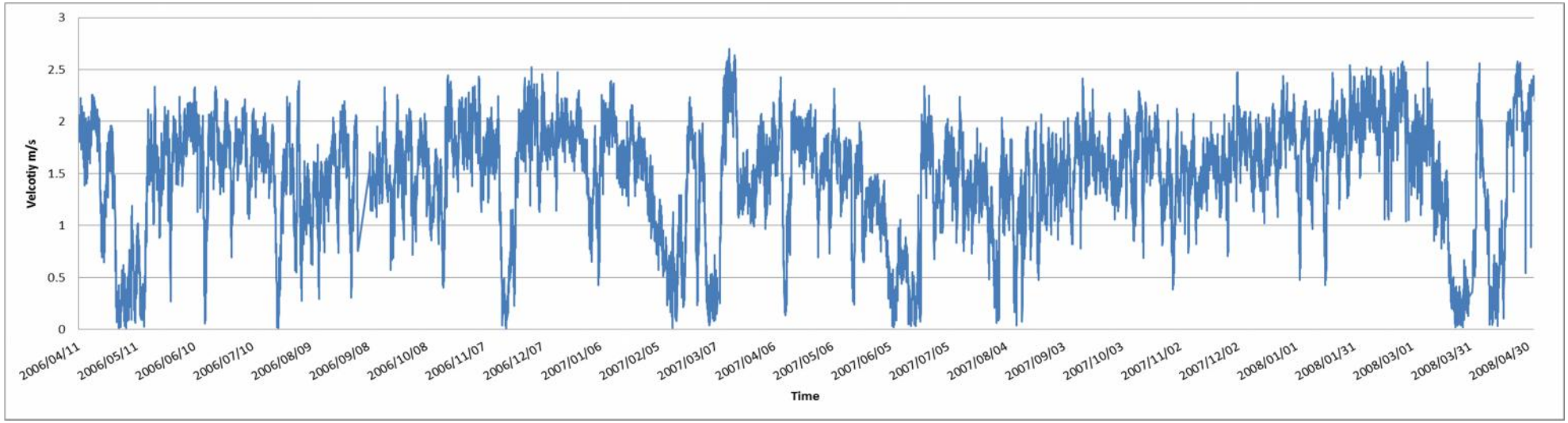

Figure 31: 24 month temporal velocity plot for East London location 1

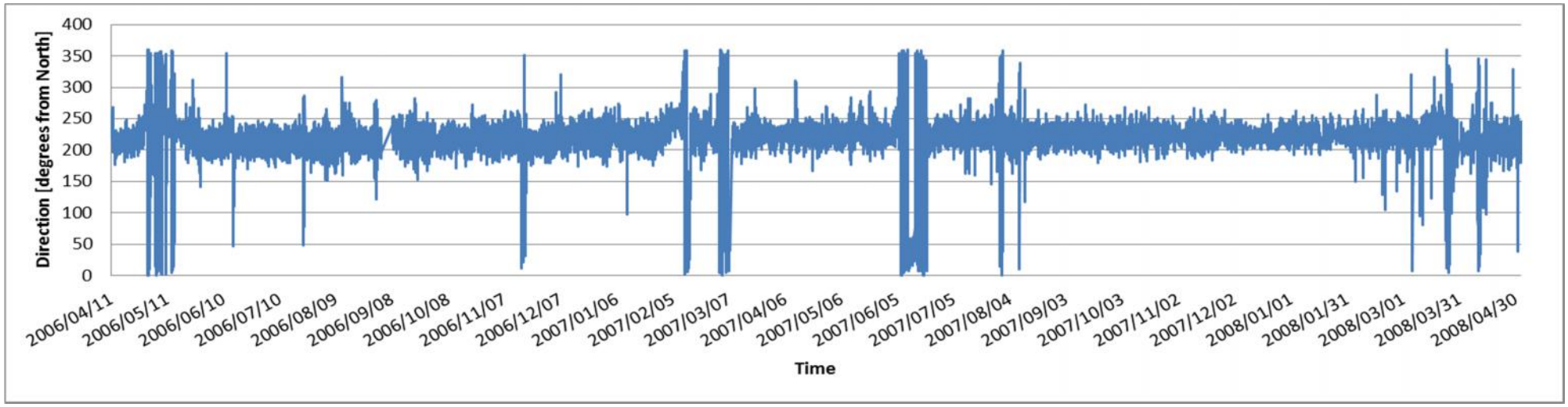

Figure 32: 24 month temporal directional plot for East London location 1

For further analysis of the variably a plot of probability of exceedance is presented in Figure 33. A summary of the findings of probability of exceedance plot can be seen in Table 16.

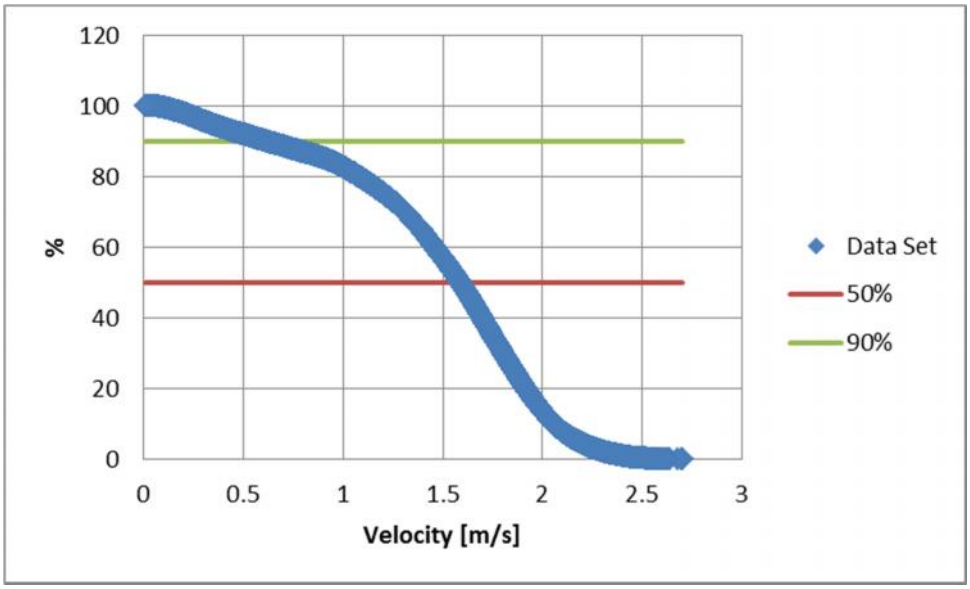

Figure 33: Exceedance of probability plot for East London location 1

Table 16: Summary of probability of exceedance for East London location 1

Probability of Exceedance	Velocity [m/s]
P50	1.59
P75	1.20
P90	0.69
P99	0.13

Figure 34 and Figure 35 show a histogram and the normal distribution plot of the velocity data.

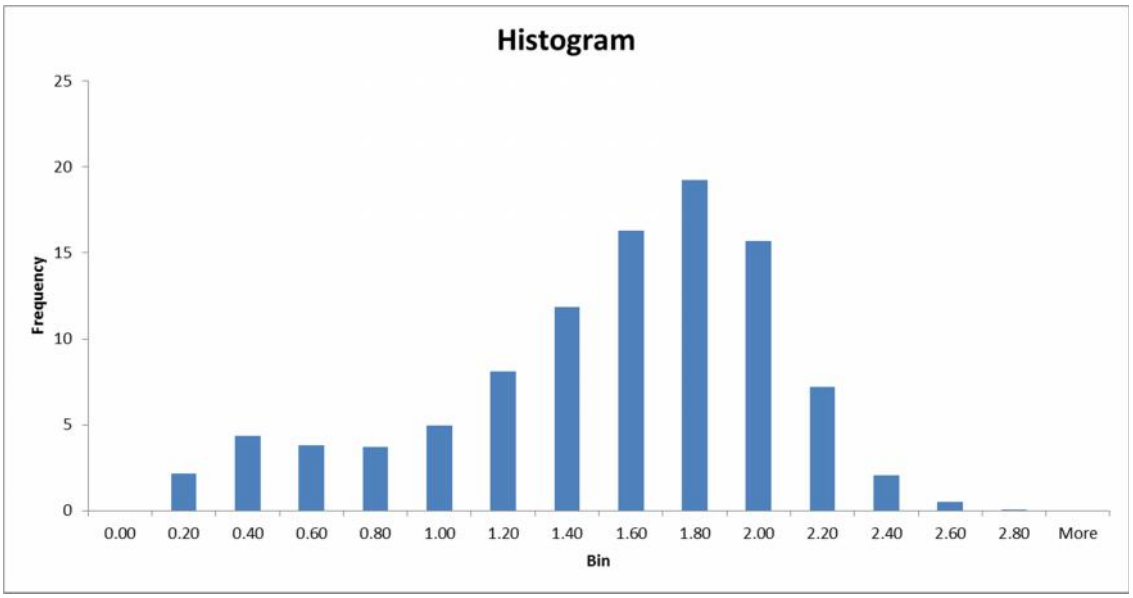

Figure 34: Histogram of velocity data

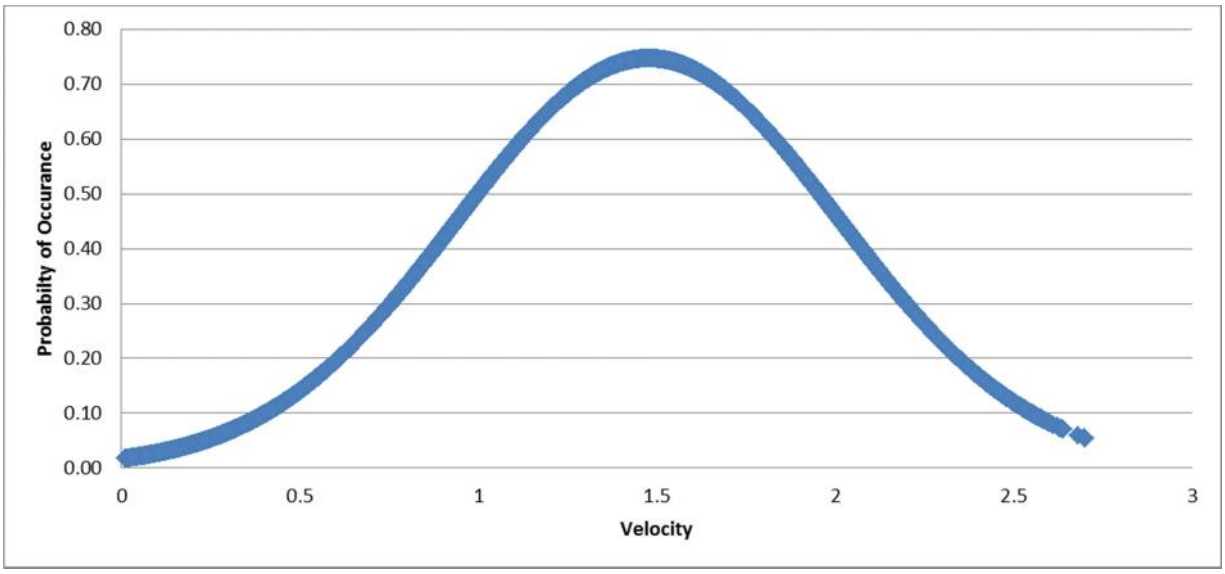

Figure 35: Normal distribution curve of velocity data

The analysis for the data at East London location 2 can be seen in Figure 36 and Figure 37. The analysis runs from 2007/08/18 to 2009/03/22. The standard deviation and mean for this data set can be seen in Table 17. It is seen that the mean velocity for this data set is less than East London location 1 and the standard deviation is higher. This large standard deviation is illustrated in Figure 36 where the velocity does not tend to a constant value even when there are no Natal Pulses present. One can see the presence of three Natal Pulses in this time period.

Table 17: East London location 2

Mean [m/s]	1.40
Median [m/s]	1.54
Mode [m/s]	1.67
Standard Deviation [m/s]	0.61
Minimum [m/s]	0.01
Maximum [m/s]	2.83

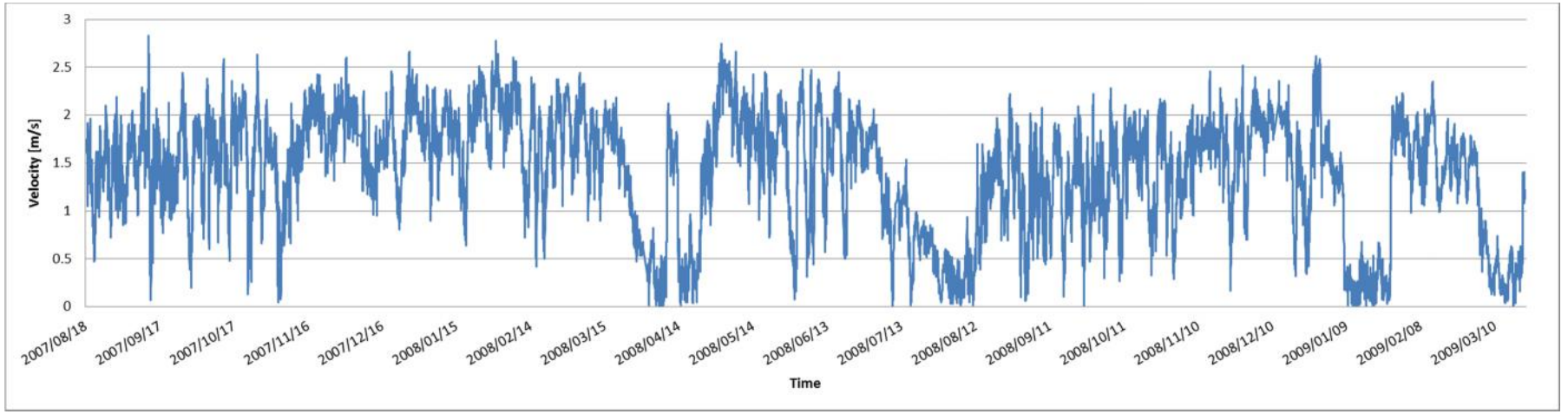

Figure 36: 19 month temporal velocity plot for East London location 2

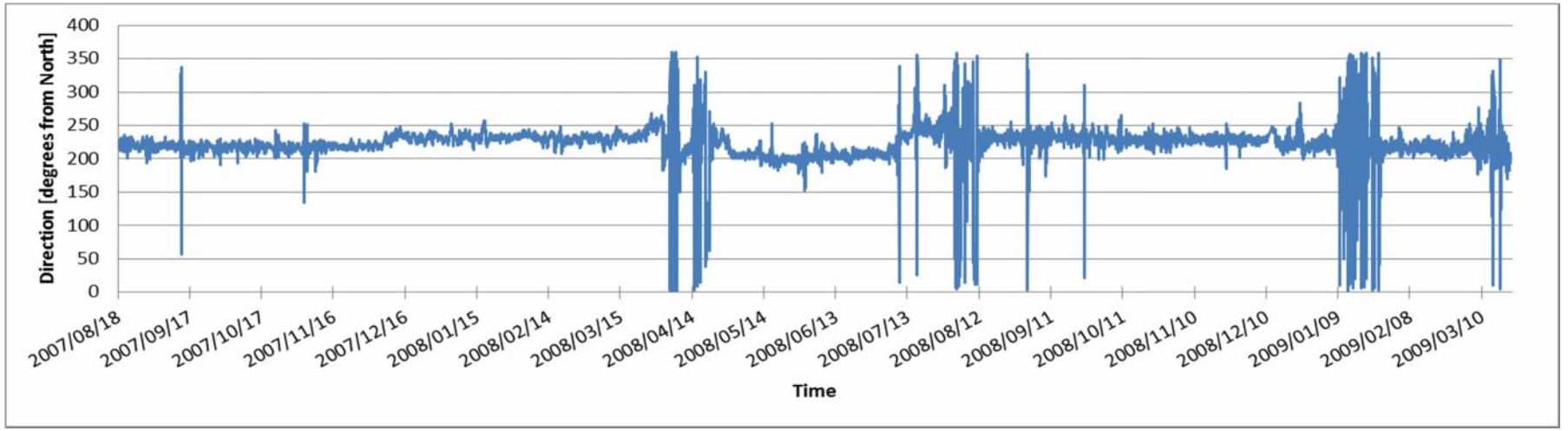

Figure 37: 19 month temporal velocity plot for East London location 2

Probability of exceedance analysis is also carried out for this location, the plot can be seen in Figure 38 and Table 18 shows the summary of probability of exceedance analysis.

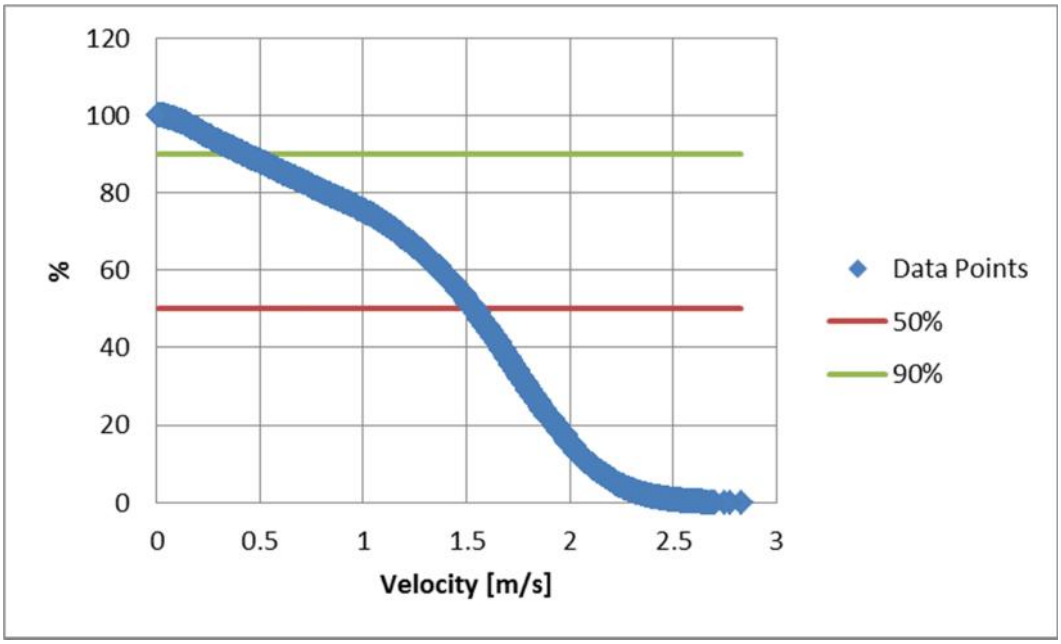

Figure 38: Exceedance of probability plot for East London location 2

Table 18: Summary of probability of exceedance for East London location 2

Probability of exceedance	Velocity [m/s]
P50	1.54
P75	1.01
P90	0.42
P99	0.09

Figure 39 and Figure 40 show a histogram and the normal distribution plot of the velocity data. Again, the presence of the low velocities seem to skew the curve.

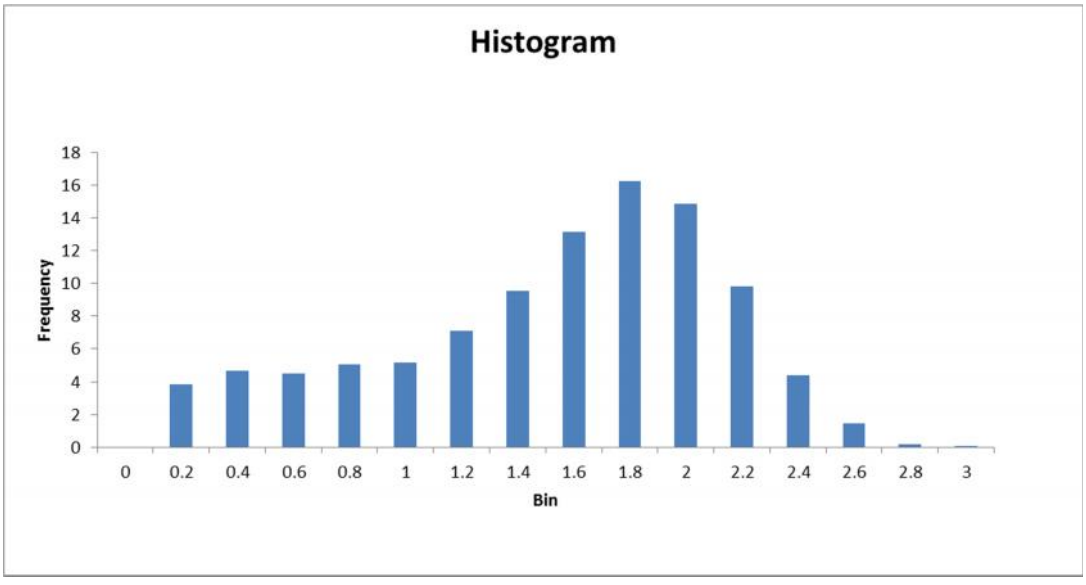

Figure 39: Histogram of velocity data

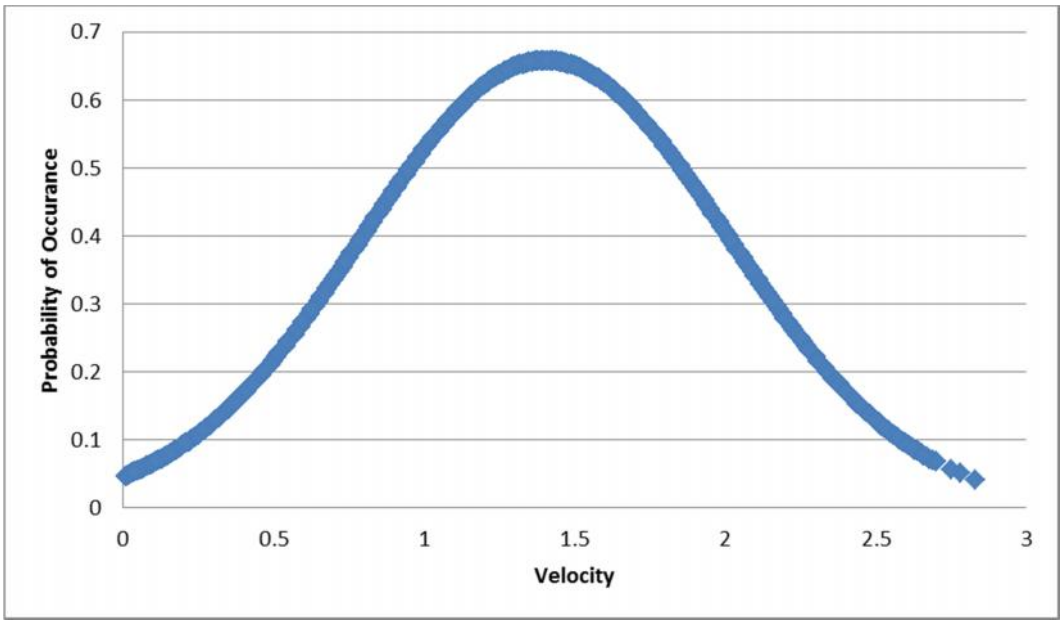

Figure 40: Normal distribution curve of velocity data

From the three time periods which have been analysed, it is seen that the direction of the current remains constant, with exception being during the passing of a Natal Pulse and the infrequent passing of a day long eddy. However, the large variation in velocity outside the regions of the Natal Pulse is worrying, thus an analysis needs to be carried out with a numerical turbine where a capacity factor can be found which will be a better indicator of the impact of the variability of the Agulhas Current.

3.3.5. Possible current performance

In order to better understand the capacity of the resource that is being analysed, a numerical turbine model is set up and the capacity factor of the Agulhas Current is examined. The capacity factor also gives a good indication of the variability of the site. Table 19 gives the numerical turbine specifications and Table 20 gives the obtained results after the numerical turbine has been implemented.

Table 19: Numerical turbine specifications

Turbine specifications	**SeaGen Turbine** (Siemens, 2012)	**Numerical Turbine**
Cut in speed	0.8 m/s	0.6 m/s
Cut out speed	2.5 m/s	2.0 m/s
C_p	0.45	0.4
Diameter	16 m	16 m

The values for the turbine are roughly based on the SeaGen turbine performance, however SeaGen turbines are designed for tidal applications which have higher average speeds and thus the cut-in and cut-out speeds are adjusted to suit the current application. Usually the SeaGen turbine with a rated power of 0.8 MW has a cut in speed of 0.8m/s and a cut out speed of 2.5 m/s, as seen in Table 19. The overall system efficiency for SeaGen has been found to be between 0.4 and 0.45 and this includes all losses in the generator, gearbox and power electronics. A value of 0.4 is to be used for the numerical turbine because, unlike for tidal applications, there is no channel blockage in the current application which can cause artificially high efficiency factors. Hence the lower efficiency factor is used.

Table 20: Achieved capacity factors and annual power produced

Site	Capacity factor %
Cape Morgan	50.9
East London location 1	50.8
East London location 2	47.5

The capacity factor achieved using the SeaGen technology (as shown in Table 19) for 1 000 operational hours is 66% (Siemens, 2012). The achieved capacity factors are considerably lower but this can be accounted for by the lower velocities experienced in current applications and the variability of the Agulhas Current. These capacity factors are however of the same order, as what is typically expected from an offshore wind farm, or perhaps slightly higher. They are also higher than onshore wind farms and PV installations.

It is seen that East London location 1 or Cape Morgan is the preferred site even though these sites are further from the nearest medium voltage station. From Figure 24, it is seen that these two sites lie 45 km and 25 km from the nearest low voltage station, respectively. The difference in capacity factor is approximately 3.3% between the two locations, but a techno-economic analysis will have to be carried out in order to see if the greater capacity power produced will compensate for the costs incurred for the longer distance of sea cabling. Figure 41 to Figure 43 show the power achieved at each site plotted with the current velocity and the power averaged over a five day period. This five day averaged power presents a smoother trend plot and highlights where the distinct drop in power occurs. It is seen that the Cape Morgan location has the smoothest averaged power curve, bar the presence of the Natal Pulses. Although East London location 1 is at the same site, the power fluctuates continually indicating the difference between the two different time periods which have been analysed for this location. However when examining plots of Figure 41 and Figure 42 it can be argued that this location is the better choice to the East London location 2 for marine turbine deployment due to the improved velocities and lower variability at this chosen site.

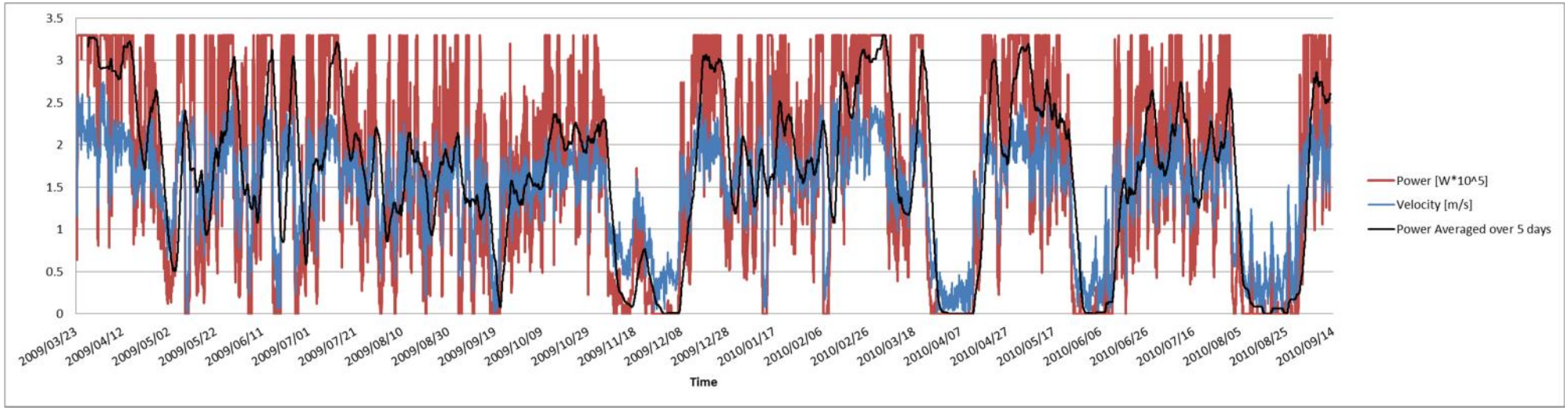

Figure 41: Cape Morgan location

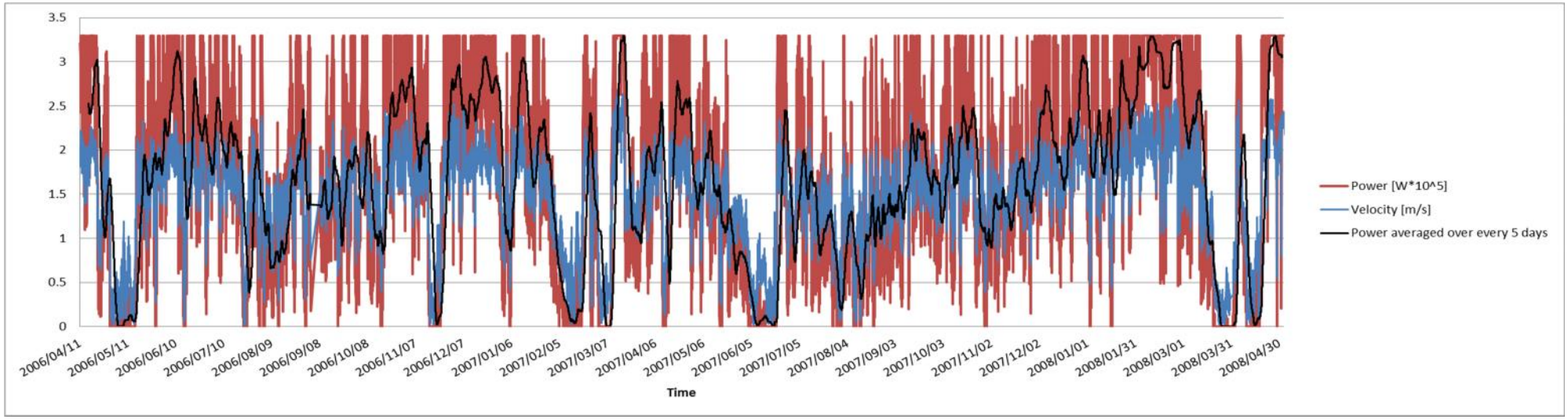

Figure 42: East London location 1

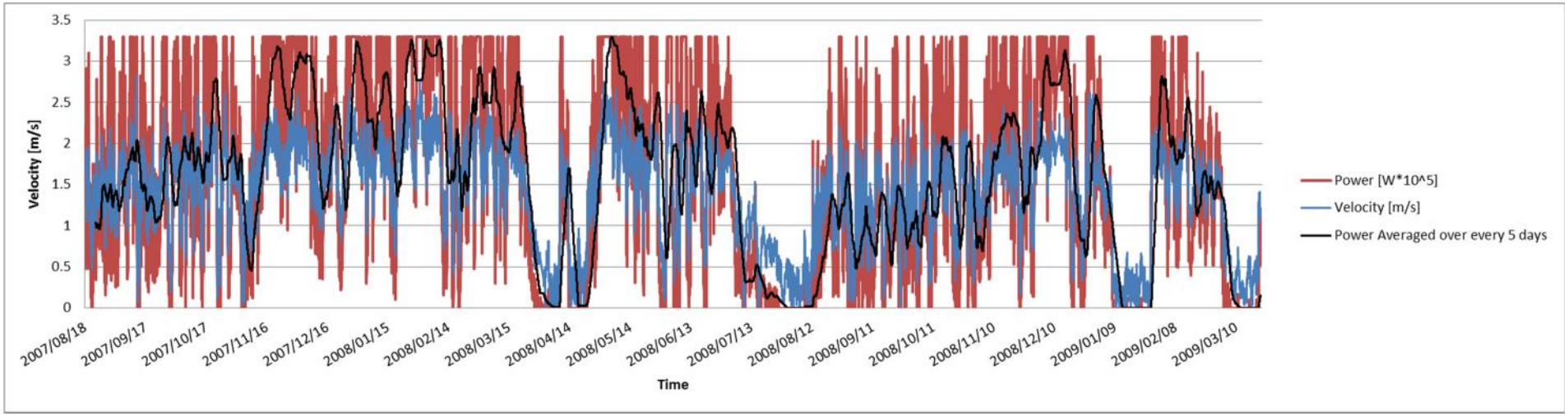

Figure 43: East London location 2

4. Conclusions and future developments

(Written by Prof J.L Van Niekerk, CRSES)

In this report the available ocean energy resource data was investigated and reported. In section 2 the available data sets, both measured and derived from satellite based measurements were presented and discussed. In section 3 the available data of the Agulhas Current was analysed to determine the potential to generate electricity from the current.

From section 2 it is clear that although a number of data sets are available, not all are readily available in the public domain. Owing to the extent of the South African coastline, there are long stretches where no measured data is available, especially measured ocean wave data. The data sets that are available need careful interpretation, especially in order to determine the available energy, and to date very little research in this area has been completed and published. From the data that is available, it does seem that South Africa does have an exploitable ocean energy resource.

From section 3 it is clear that the Agulhas Current can be seen as an attractive source of renewable energy but due to variations in both the speed and direction of the current, it cannot be considered to be a constant (base-load) supply of energy. This is due to the current meandering as well as anomalies such as the Natal Pulses that can even reverse the direction of the current at a specific location. The computed capacity factors of just more than 50% at East London and Cape Morgan are however still high for a variable, renewable energy resource that could warrant exploitation, provided suitable technology can be developed to do this in a cost-effective manner.

From this study, it is clear that although a large body of knowledge on the wave conditions along the South African coast exists, as well as data on the Agulhas Current, there are numerous gaps that need to be filled. It is also interesting to note that there are three main groups interested in this data; oceanographers, harbour and shipping operators, and parties interested in exploiting the resource for renewable energy. It is however not clear if there is sufficient communication and sharing of data between these different groups and what the effect of such cooperation may be.

Based on the results of this report, the following conclusions and recommendations can be put forward:

- Although there are a number of different data sources and sets available at this time there are still many gaps. There is also a lack of coordination between the different stakeholders. It will be very useful if a process can be initiated to bring the different stakeholders together to discuss cooperation and sharing of resources and data. It is recommended that such a process be initiated by one of the interested parties.
- There is clearly a significant amount of energy available in the Agulhas Current but harnessing it remains a technical challenge. The variability of the current, which may be more than what was expected, will also reduce the amount of electricity that can be generated and the attractiveness of the current as a constant (base-load) source of energy. The next step in this investigation will be to consider the existing ocean current technology available to generate electricity from this source and to consider

how it could be adapted and implemented at one or more of the identified sites. This will need to be done as part of a detailed techno-economic analysis.

- (A more detailed study of the wave energy resource will be presented in a separate report with suitable recommendations on the wave energy resource.)

5. References

Beal, L. (2003): The Agulhas Undercurrent Experiment. [Online] Available at: http://www.po.gso.uri.edu/wbc/Fall_Beal/ [Accessed 20 02 2013].

Beal, L.M. and H.L. Bryden (1997): Observations of an Agulhas Undercurrent. *Deep-Sea Res. I*, 44, 1715–1724.

Beal, L.M. and H.L. Bryden (1999): The velocity and vorticity structure of the Agulhas Current at 32°S. *J. Geophys. Res*., 5151–5176.

Bryden, H. L., Beal, L. M. & Duncan, L. M. (2005). Structure and Transport of the Agulhas Current and Its Temporal Variability. *Journal of Oceanography,* 61, 479 - 492.

Chang C and J Curlander (1992). Application of the multiple PRF technique to resolve Doppler centroid estimation ambiguity for spaceborne SAR, IEEE Trans. Geosci. Remote Sensing 30: 941–949.

Chapron B, Collard F, and V Kerbaol (2004). Satellite synthetic aperture radar sea surface Doppler measurements. In Proceedings of the Second Workshop on Coastal and Marine Applications of SAR, Eur. Space Agency Spec. Publ., ESA S-565: 133–140.

Collard F, Mouche A, Chapron B, Danilo C and JA Johannessen (2008). Routine high resolution observation of selected major surface currents from space. A paper presented at Workshop SEASAR 2008, Eur. Space Agency, Frascati, Italy.

CSIR (2003). Offshore potential for power generation: A preliminary study of ocean currents and associated offshore marine environment off the east coast of South Africa. CSIR report 3RE-000093, Stellenbosch, 102 pp.

De Ruijter, W.M.P., Beal, L., Biastoch, A. and Zahn, R. (2013) The Role of the Agulhas System in Regional and Global Climate AGU Chapman Conference: The Agulhas System and Its Role in Changing Ocean Circulation, Climate, and Marine Ecosystems; Stellenbosch, South Africa, 8–12 October 2012. *Eos*, Vol. 94, No. 10, 5 March 2013.

Donohue, K.A. Firing, E. and L. Beal. (2000). Comparison of three velocity sections of the Agulhas Current and Agulhas Undercurrent. Journal of Geophysical Research, 105: 28 585–28 595.

Duncan, C.P. (1976). High waves in the Agulhas Current. mariners Weather Log, 20(1), 1–5.

Elombo, A., Chowdhury, S. & Chowdhury, S. (2010) Design Context for Tidal Current Energy: The Agulhas Current Stream. *IEEE International Energy Conference*.

Goldstein RM, and HA Zebker (1987). Interferometric radar measurement of ocean surface currents. *Nature* 328: 707–709.

Gyory, J., Mariano, A. J. & Ryan, E. H., (2012). The Benguela Current. [Online] Available at: http://oceancurrents.rsmas.miami.edu/atlantic/benguela.html [Accessed 11 03 2013].

Hasselmann K., and Hasselmann, S. (1991). On the nonlinear mapping of an ocean wave spectrum into a synthetic aperture radar image spectrum and its inversion, *Journal of Geophysical Research*, C96:10,713–10,729.

Johannessen JA, Chapron B, Collard F, Kudryavtsev V, Mouche A, Akimov D and KF Dagestad (2008). Direct ocean surface velocity measurements from space: Improved quantitative interpretation of Envisat ASAR observations, Geophysical Research Letters 35: L22608, doi:10.1029/2008GL035709.

Komen, G.J., Cavaleri, L., Donelan, M., Hasselmann, K., Hasselmann, S. and Janssen, P.E.E.M. (1994). Dynamics and modelling of ocean waves, *Cambridge University Press*, Cambridge, 532 pp.

Lutjeharms J. (2006). The Agulhas Current. New York: Springer

Madsen SN (1989). Estimation the Doppler centroid of SAR data, *IEEE Trans*. Aerospace Electronic Systems 25: 134–140.

Moodley, R (2011). Technological Analysis and Feasibility Study of Pilot and Commercial Marine Power PLants for Energy Extraction from the Agulhas Current, Cape Town: University of Cape Town, Department of Electrical Engineering.

Roberts, M.J., van der Lingen, C.D., Whittle, C. and M van den Berg (2010). Shelf currents, lee-trapped and transient eddies on the inshore boundary of the Agulhas Current, South Africa: their relevance to the KwaZulu-Natal sardine run *Roberts African Journal of Marine Science* 2010, 32(2): 423–447

Romeiser R, Breit H, Eineder M, Runge H, Flament P, de Jong K and J. Vogelzang (2005). Current measurements by SAR along-track interferometry from a space shuttle, *IEEE Trans*. Geosci. Remote Sensing 43, 2315–2324.

Rossouw, J. (1989). Design waves for the South African Coastline. PhD thesis, University of Stellenbosch, Stellenbosch, South Africa.

Rossouw, M, Davies, J, Coetzee, L. and Kuipers, J. (1999). The Wave Recording Network around the South African Coast. Proceedings of the 5th International Conference on Coastal and Port Engineering in Developing Countries (COPEDEC). Cape Town, South Africa, April 1999.

Rossouw, M and Von St. Ange, U (2011). Overview of Wave Conditions around South African Coast. CSIR Report – Draft.

Rouault, M. (2011). Agulhas Current variablility determined from space: a multi-sensor approach, Cape Town: University of Cape Town.

Rouault MJ, Mouche A, Collard F, Johannessen JA and Chapron B. (2010). Mapping the Agulhas Current from space: An assessment of ASAR surface current velocities. *Journal of Geophysical Research*, 115: C10026, doi:10.1029/2009JC006050.

Schumann EH. (1982). Inshore circulation of the Agulhas Current off Natal. *Journal of Marine Research* 40: 43–55.

Schumann EH. (1988). Physical oceanography of Natal. In: Schumann EH (ed.), Lecture notes on coastal and estuarine studies. New York: Springer-Verlag, pp 101–130.

Shemer L, Marom M and D Markman (1993). Estimates of currents in the nearshore ocean region using interferometric synthetic aperture radar. *Journal of Geophysical Research* 98: 7001–7010.

Siemens, (2012). Marine Current Turbines. [Online] Available at: http://www.seageneration.co.uk/ [Accessed 20 02 2013].

Toole, J.M. and B.A. Warren, (1993): A hydrographic section across the subtropical South Indian Ocean. Deep-Sea Research I, 40: 1973–2019.

Vesecky, J.F., and Stewart, R.H. (1982) The observation of ocean surface phenomena using imagery from the Seasat synthetic aperture radar: An assessment. *Journal of Geophysical Research*, Vol. 87(C5): 3397–3430.

Vignudelli S, Berry P and L Roblou (2008). Satellite altimetry near coasts: Current practices and a look at the future. A paper presented at 15 Years of Progress in Radar Altimetry, European Space Agency, Venice, Italy.

Whillier (1962). Ocean currents at East London. Transactions of the South African Institute for Civil Engineering, January 1962: 1–7.

Wright, S., Chowdhury, S. & Chowdhury, S., (2011). A Feasibility Study for Marine Energy Extraction from the Agulhas Current. *IEE.*

Appendix A

Agulhas Current ADCP data

A total of 51 deployments were made between September 2005 and September 2010. The details of each deployment, including deployment date and time, GPS position and instrument type are given in Table 1.

The files are grouped into five main directories, according to the area of deployment – Cape Morgan, East London, Fish River or Port Edward (See Figure 1 for deployment area.) The main directory 'East London_Nortek' contains data collected near East London with a Nortek ADCP.

Inside each main directory there are 2 subdirectories – ADCP currents and Bottom temperature.

The data is given in bins that divide the water column into horizontal sections.

- only bins where less than 25 % of the current measurements were labeled as 'bad data' are included.
- Bin 1 is always closest to the ADCP, with consecutive numbers moving away from the ADCP.
- Depth is the actual or calculated depth in meters of the center of that bin.
- Range is the distance in meters from the ADCPs transducer to the center of that bin.
- Readme files contain information on missing data for that deployment.

Table A.1: Deployment details for ADCP current meter deployments made on the east coast of South Africa.

SQ	Filename	ADCP type	Pressure sensor	Latitude (S)	Longitude (E)	Deployment date	Recovery date	Ship sounding (m)	Position
1	PE751	RDI 75	yes	-31.22263	30.20273	8-Sep-2005 16:44	11-Dec-2005 10:25	156	offshore
2	PE301	RDI 300 + waves	yes	-31.19722	30.17517	8-Sep-2005 17:06	11-Dec-2005 11:20	60	midshelf
3	PE601	RDI 600	yes	-31.17855	30.15253	8-Sep-2005 17:30	11-Dec-2005 12:05	31.8	inshore
4	PE602	RDI 600	**no**	-31.17860	30.15263	11-Dec-2005 13:58	10-Apr-2006 10:40	32.98	inshore
5	PE302	RDI 300 + waves	yes	-31.19732	30.17480	11-Dec-2005 14:54	10-Apr-2006 09:36	61.74	midshelf
6	PE752	RDI 75	yes	-31.22303	30.20270	13-Dec-2005 17:02	06-Apr-2006 08:22	173.4	offshore
7	EL1901	Nortek	yes	-32.50997	28.83000	14-Dec-2005 02:15	07-Apr-2006 09:10	83.25	midshelf
8	PE603	RDI 600	yes	-31.17865	30.15245	10-Apr-2006 17:30	09-Sep-2006 09:00	32.11	inshore
9	PEM03	RDI 600	**no**	-31.19753	30.17460	10-Apr-2006 17:50	09-Sep-2006 08:30	62.11	midshelf
10	EL201	Nortek	yes	-32.50717	28.83242	11-Apr-2006 14:45	02-Sep-2006 16:00	82.95	midshelf
11	EL303	RDI 300 + waves	yes	-32.32363	29.02225	11-Apr-2006 17:10	02-Sep-2006 07:00	96	midshelf
12	EL403	RDI 75	yes	-32.96595	28.30622	1-May-2006 19:06	08-Sep-2006 06:45	96	midshelf
13	EL754	RDI 75	yes	-32.57633	28.75208	8-Sep-2006 14:55	12-Dec-2006 08:40	91.99	midshelf
14	EL301	Nortek	yes	-32.50763	28.83210	8-Sep-2006 15:55	12-Dec-2006 10:45	84.78	midshelf
15	EL304	RDI 300	yes	-32.47545	28.79237	8-Sep-2006 16:27	12-Dec-2006 11:45	90	midshelf
16	EL401	Nortek	yes	-32.50753	28.83292	13-Dec-2006 11:28	07-Mar-2007 13:26	81.3	midshelf
17	EL755	RDI 75	yes	-32.64985	28.69545	13-Dec-2006 14:57	07-Mar-2007 15:25	102	offshore
18	EL305	RDI 300	yes	-32.87433	28.43367	13-Dec-2006 20:26	07-Mar-2007 18:02	88.8	midshelf
19	EL501	Nortek	yes	-32.50743	28.83293	8-Mar-2007 06:29	17-Aug-2007 15:34	85.5	midshelf
20	EL756	RDI 75	yes	-32.43732	28.94465	8-Mar-2007 08:45	17-Aug-2007 17:05	196	offshore
21	EL306	RDI 300	yes	-33.15012	28.11602	8-Mar-2007 14:49	14-Aug-2007 11:26	98.7	midshelf
22	EL601	Nortek	yes	-32.50735	28.83287	18-Aug-2007 10:20	06-Dec-2007 15:40	84.84	midshelf
23	EL757	RDI 75	yes	-32.51000	28.83287	18-Aug-2007 10:37	06-Dec-2007 14:52	83.86	midshelf
24	EL307	RDI 300	yes	-33.15005	28.09953	18-Aug-2007 15:19	06-Dec-2007 06:45	83.5	midshelf
25	FR301	RDI 300	yes	-33.85170	27.08120	18-Aug-2007 21:33	05-Dec-2007 16:44	89.6	midshelf
26	EL701	Nortek	yes	-32.50802	28.83293	07-Dec-2007 17:47	30-Mar-2008 08:20	85	midshelf

27	EL308	RDI 300	yes	-33.14983	28.09905	07-Dec-2007 21:07	30-Mar-2008 16:00	85	midshelf
28	FR752	RDI 75	yes	-33.85070	27.08023	08-Dec-2007 01:30	29-Mar-2008 08:30	88	midshelf
29	EL801	Nortek	yes	-32.50754	28.83314	01-Apr-2008 06:05	12-Jul-2008 07:30	87	midshelf
30	EL309	RDI 300	no	-33.14990	28.09933	01-Apr-2008 11:24	11-Jul-2008 15:03	88.7	midshelf
31	FR303	RDI 300	yes	-33.70283	27.29817	1-Apr-2008 16:01	13-Jul-2008 07:24	97	midshelf
32	EL310	RDI 300	yes	-33.14970	28.09903	11-Jul-2008 16:32	10-Dec-2008 17:30	82	midshelf
33	EL901	Nortek	yes	-32.50495	28.83143	12-Jul-2008 13:45	13-Dec-2008 06:50	84.5	midshelf
34	CM301	RDI 300	yes	-32.50737	28.83185	12-Jul-2008 14:06	13-Dec-2008 06:05	82.7	midshelf
35	FR304	RDI 300	no	-33.70290	27.29782	13-Jul-2008 09:41	09-Dec-2008 08:30	96	midshelf
36	FR305	RDI 300	no	-33.70310	27.29803	12-Dec-2008 09:38	4-Feb-2009 03:57	91.72	midshelf
37	EL311	RDI 300	yes	-33.15115	28.09700	12-Dec-2008 17:25	22-Mar-2009 08:30	83.12	midshelf
38	EL1910	Nortek	yes	-32.50560	28.83183	13-Dec-2008 13:23	23-Mar-2009 09:20	86	midshelf
39	CM302	RDI 300	yes	-32.49923	28.82348	13-Dec-2008 13:41	23-Mar-2009 10:10	86	midshelf
40	FR306	RDI 300	yes	-33.70322	27.29727	21-Mar-2009 14:20	24-Aug-2009 08:20	91.5	midshelf
41	EL312	RDI 300	yes	-33.15160	28.08072	23-Mar-2009 11:10	26-Aug-2009 07:20	86.6	midshelf
42	CM303	RDI 300	yes	-32.50638	28.83150	23-Mar-2009 11:10	25-Aug-2009 08:07	83.7	midshelf
43	CM304	RDI 300	no	-32.50790	28.83100	25-Aug-2009 09:15	5-Dec-2009 10:37	83	midshelf
44	EL313	RDI 300	yes	-33.15203	28.08727	26-Aug-2009 08:54	4-Dec-2009 14:30	82.7	midshelf
45	FR307	RDI 300	yes	-33.70333	27.29677	26-Aug-2009 15:24	4-Dec-2009 06:20	84	midshelf
46	EL314	RDI 300	yes	-33.15145	28.00866	4-Dec-2009 14:58	3-Mar-2010 13:15	89.02	midshelf
47	FR308	RDI 300	yes	-33.70335	27.29750	4-Dec-2009 20:06	4-Mar-2010 06:50	93.3	midshelf
48	CM305	RDI 300	no	-32.50733	28.83183	5-Dec-2009 13:39	3-Mar-2010 06:20	85.94	midshelf
49	CM306	RDI 300	no	-32.50725	28.83179	3-Mar-2010 09:10	13-Sep-2010 06:45	84	midshelf
50	EL315	RDI 300	yes	-33.15140	28.08651	3-Mar-2010 15:25	13-Sep-2010 11:30	88	midshelf
51	FR309	RDI 300	yes	-33.71332	27.29745	4-Mar-2010 08:15	3-Sep-2010 15:50	93.2	midshelf

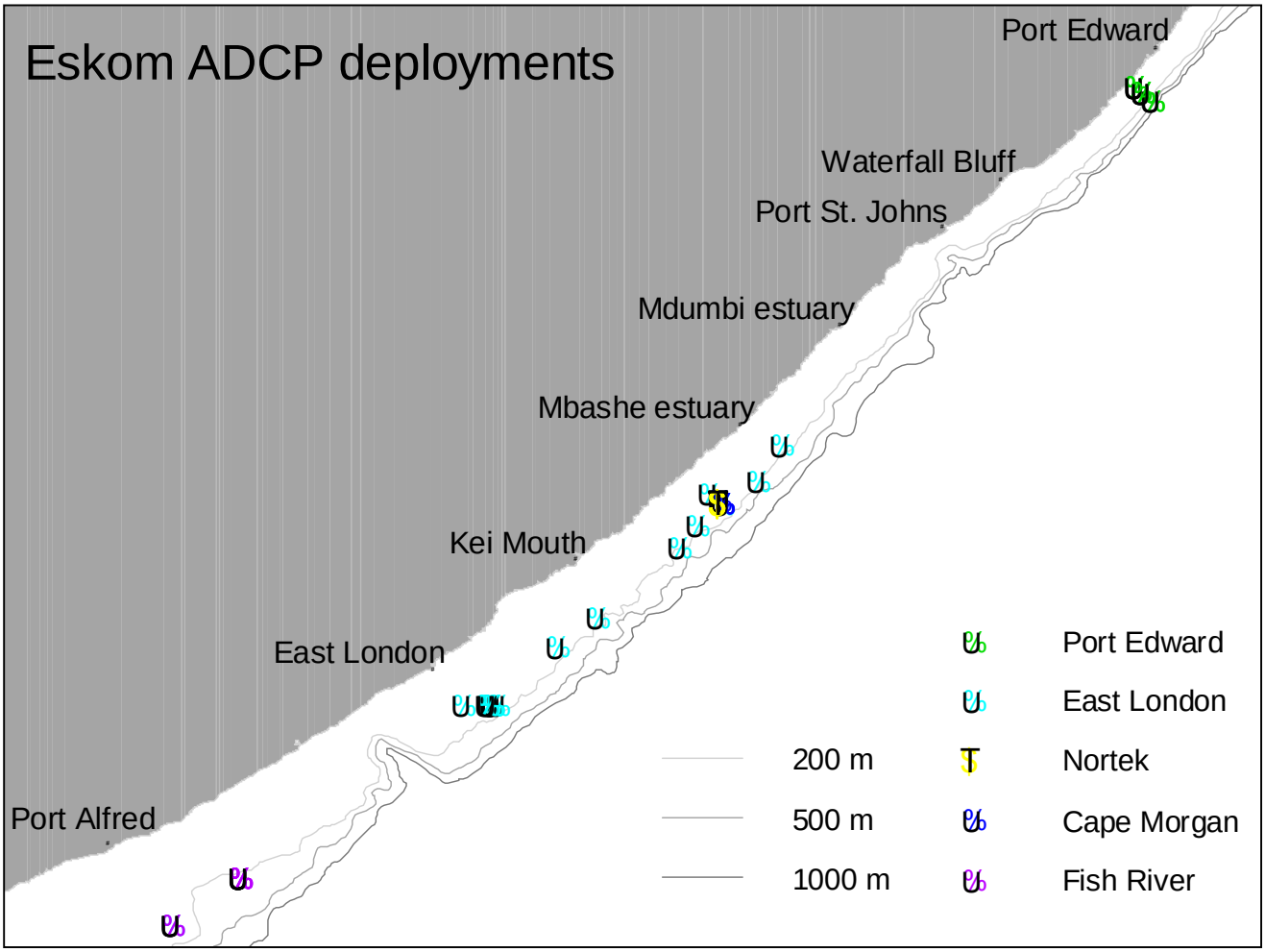

Map of ADCP deployments made on the south coast of South Africa between September 2005 and September 2010.

Appendix B

Wave data have been collected around the Southern African coasts since about 1940. The first wave observations were made from merchant vessels which travelled around the coast — the so-called Voluntary Observing Ships (VOS). From these ships visual estimates were made regularly of wave heights, periods and directions. These observations were later augmented by wave recordings made with a variety of instruments including clinometers, ship-borne wave records, pressure meters, inverted echo-sounders and accelerometer buoys.

Wave data for use in coastal engineering projects in South Africa were first collected by means of a wave clinometer off the Bluff at Durban in 1961. The wave clinometer consists of a telescope having graduations on one lens through which nearshore wave direction is observed from a high vantage point on the shore. Visual estimates of wave height and wave period was also made by observing the movements of a moored buoy through the graduated lens of the telescope. During the period 1964 to 1969, the research ships Africana II, Thomas B Davie, Meiring Naudé and Benguela, as well as the survey vessel SAS Natal, were fitted with NIO ship-borne wave recorders. These recorders, which used a combination of accelerometers and pressure recorders, were fitted to the ship's hull and gave as output an analogue trace of the water surface from which wave-height and wave-period data were extracted. Wave directions were estimated visually from the bridge of the ship by means of the ship's compass.

South Africa also operated a weather ship, the F H Hughes, during the period September 1969 to March 1974. The ship was usually stationed off Cape Point at 40° S; 10° E and was first fitted with a Boersma recorder which was later replaced by a NIO recorder.

In February 1967 a wave research group was established within the National Mechanical Engineering Research Institute (NMERI) of the CSIR with the main aim of recording and statistically analysing wave conditions along the coastlines of South Africa and South West Africa (Namibia). This so-called "Ocean Wave Research Project" was initiated by the South African National Committee for Oceanographic Research (SANCOR) with financial support and guidance from SANCOR, VISKOR, SOEKOR and NMERI.

The main wave recording instrument used during the period 1961 to 1970 was the wave clinometer. The number of wave clinometer stations increased from one in 1965 to twelve in 1970. The wave clinometer stations remained in service until late in 1974.

In an attempt to increase the accuracy of the visually measured wave data obtained by the clinometer, a number of wave recording instruments were experimented with during the period 1966 to 1969. First an inverted echo-sounder (Kelvin Hughes), connected by cable to shore, was tried in Cape Town and Durban. This experiment was eventually abandoned mainly because of difficulties with the laying and maintenance of the cable through the surf-zone. A self-contained inverted echo-sounder (INES) was developed and used for a while, but it suffered from many internal defects and leakage problems. Eventually it fell into disuse without producing many useful results. A few pressure recorders (OSPOS) were bought from Van Essen in Holland by NMERI and VISKOR. This self-contained unit proved to be very reliable. The records were, however, difficult to analyse and doubts were expressed regarding the transfer functions used to convert the pressure-record to a water-surface record.

In July 1969 an accelerometer buoy, the Datawell Waverider was installed in 100 m water depth off Mossel Bay. The moored buoy transmitted to shore where the data were recorded. Initially a paper tape recorder was used, but it never functioned satisfactorily and later recordings were made on a strip-chart recorder. The Waverider soon proved to be superior to any of the wave recorders tried previously and, during the period 1971 to 1973, the number of Waverider stations was increased from one to seven. All of these stations recorded waves in analogue form on paper rolls, usually for 20 minutes every six hours. All analysis had to be done by hand and by late 1974 the backlog in analysis became so large that it was decided to reduce the number of Waverider stations to those required for urgent coastal engineering studies until instrumentation and software could be developed for recording in computer-compatible form. The first digital recorder was installed at Slangkop off the Cape Peninsula in February 1976. Digital recordings were made on a cassette tape, typically with a capacity of 10 days' worth of four recordings per day.

Although the digital recordings could now be quickly processed by computer, the need was recognised to develop software which would check the quality of the data without having to display or plot the individual recordings and rely on human judgement as to its integrity. A joint project was launched by the Institute of Maritime Technology (IMT) and the National Research Institute for Oceanology (NRIO, CSIR) and in 1980 a computer program was produced which efficiently analyses and checks wave recordings for quality. A computerized database was also established for storage and retrieval of all the wave records, which had passed the quality checks.

Recording on cassette proved to have several drawbacks. Recording stations had to be situated at manned locations to facilitate changing and mailing the cassettes to the CSIR in Stellenbosch. Cassettes were sometimes lost or damaged and often accumulated at the recording site. The result was that often bad recordings and lost Waveriders were only discovered many weeks later with resultant loss in data and equipment. With the advent of the PC-era, a solid-state data-logger was developed and connected, via dial-up modem, to a PC-based base station at Stellenbosch. Software was developed which automatically collected and analysed the data on an around-the-clock basis. This system became fully operational around 1985.

Work also continued to locally produce an accelerometer buoy. The final product *Wavemonitor* was developed and successfully implemented around 1993.

Although the accelerometer buoy has virtually become the standard wave-recording instrument in South Africa, it does not measure wave direction. During the early 70's VISKOR developed the DOSO. This instrument sensed the direction of the orbital motions of the waves and is normally placed on the sea-bottom in a water depth of less than 20 m. Useful shallow water data were obtained from the DOSO at a few sites in South Africa such as Koeberg and Gansbaai. Radar was also used to record nearshore wave direction at Koeberg and useful (although intermittent) information was obtained by analysis of photographs of the image on the radar screen. Since the DOSO and radar were used to measure waves in relatively shallow water, refraction techniques were required to obtain the more generally applicable deep-sea wave direction.

Field experiments were also conducted with commercially available directional wave buoys. Between 1986 and 1992 field tests were done with an Endeco Type 956 Wavetrack buoy and a Datawell directional Waverider buoy. The data from these two buoys were compared to those of an electromagnetic currentmeter (EMCM) placed underneath the buoys. Results indicated that the directional Waverider and the EMCM compared well. It was established that the Endeco buoy had

difficulty in resolving the directional wave spectrum in a swell dominated wave climate such as around the South African coast.

Although non-directional Waverider and Wavemonitor buoys were mainly used, there was a growing need for real-time directional wave information. At the time, the CSIR successfully developed a directional wave buoy using standard GPS technology called the 3D buoy.

Directional measurements commenced in 1997 off East London and later off Richards Bay and Cape Town. However, due to poor continuous satellite coverage at the time, the buoys were replaced with Datawell directional Waveriders. Bottom-mounted systems were also acquired. A Teledyne RD Instruments ADCP has been operating on a real-time basis since 2002 off the Port of Durban. This system provided information on the ocean currents as well as the wave conditions.

As the need grew for the real-time data, the basic wave recording had to be automated in order to provide an efficient and cost-effective system to all the major South African ports. The development of this system led to the wave-recording network (Wavenet) whereby the data from the wave stations around the South African coast could be effectively managed.